Titre: Title:	Printability and Electrical Response of the Sepia Melanin Bio-Pigment on Paper for Sustainable Printed Electronics
Auteur: Author:	Camille Bour
Date:	2023
Type:	Mémoire ou thèse / Dissertation or Thesis
Référence: Citation:	Bour, C. (2023). Printability and Electrical Response of the Sepia Melanin Bio-Pigment on Paper for Sustainable Printed Electronics [Master's thesis, Polytechnique Montréal]. PolyPublie. https://publications.polymtl.ca/55117/

URL de PolyPublie: PolyPublie URL:	https://publications.polymtl.ca/55117/
Directeurs de recherche: Advisors:	Clara Santato
Programme: Program:	Génie des matériaux

POLYTECHNIQUE MONTRÉAL

affiliée à l'Université de Montréal

Printability and electrical response of the Sepia melanin bio-pigment on paper for sustainable printed electronics

CAMILLE BOUR

Département de génie physique

Mémoire présenté en vue de l'obtention du diplôme de *Maîtrise ès sciences appliquées*

Génie des matériaux

Août 2023

POLYTECHNIQUE MONTRÉAL

affiliée à l'Université de Montréal

Ce mémoire intitulé :

Printability and electrical response of the Sepia melanin bio-pigment on paper for sustainable printed electronics

présenté par **Camille BOUR**

en vue de l'obtention du diplôme de *Maîtrise ès sciences appliquées*

a été dûment accepté par le jury d'examen constitué de :

Julian SELF, président
Clara SANTATO, membre et directrice de recherche
Lucien WEISS, membre

DEDICATION

I would like to thank every person that contributed to this work and helped me to begin this wonderful adventure exploring the Sepia melanin possibilities and opportunities.

J'aimerais remercier toutes les personnes de près ou de loin qui m'ont permis d'entreprendre ce chemin, de faire ce que je fais, et d'être la personne que je suis aujourd'hui. Je remercie ma famille pour son soutien. Je remercie mes amis, qui me manquent, mais malgré la distance et le temps qui court, demeurent présents et me donnent toujours autant le sourire. Merci à Inès et Camille et félicitations pour vos parcours, tout cela est tellement beau. Merci à mes amis de Prépa, à tous ces merveilleux moments passés pendant et après ces deux années : Marina, Anna, Alexandre et Ophélie. Merci à mes amis rencontrés en école d'ingénieur pour ces expéditions et moments de bonheur dans le magnifique bassin Isérois : Nicolas, Renaud, Romain, Loïs et Emilie. Obrigada to my Brazilian friends Lariel, Luan and Mara for their warmth and the smile they always put on my face. Gracias Yasser por todos : la sua amistad y ayuda. Merci beaucoup à Anthony, Joaquin et Manuel, apprendre à vos côtés a été incroyable. Et, non des moindres, merci à mon équipe toujours présente en vocal pour les moments de rire et de joie qui m'ont énormément soutenue, sans même le savoir, dans les moments difficiles loin de mes proches : Anthony, Angelo, Chris, Stevens, Diyar, Alexis et Hadrien. E grazie specialmente a te Antonio, sai perché. Je remercie mes anciens professeurs, de tout niveau et de toutes matières, qui m'ont encouragée et apporté une aide précieuse durant mes études et parfois aussi personnellement. Merci aux professeurs de Pagora et Polytechnique. Grazie Clara per il tuo aiuto e la possibilità che mi dai. Grazie per il tuo supporto dentro e fuori Polytechnique. Enfin je voulais remercier ma famille proche, ma grand-mère pour son courage, ce que tu as fait pour nous. Merci à Donato et Océane pour la magnifique famille qu'on forme. Merci à toi Donato pour tout ce que tu m'as appris, ton soutien et tes précieux encouragements. Merci à toi Océane, je suis tellement fière de ce que tu fais, de ton parcours et de la personne que tu es. Une pensée à mon grand-père, ces études étaient pour toi aussi, j'aurais aimé que tu puisses en contempler la fin. Et bien sûr, un merci inconditionnel à celle qui a réalisé tous les efforts nécessaires pour que j'en sois là, ma confidente, maman, malgré tout ce qui s'est passé. Tu as toujours fait le nécessaire, j'espère que tu seras fière. Merci à Patricia, Christelle et Sandrine.

ACKNOWLEDGEMENTS

I thank Professor Julian Self and Professor Lucien Weiss for their acceptance as jury president and member. I am grateful for this opportunity. It is an honor to be able to present this work with a core subject that stems from years of study in our research group. I also thank them for their precious advice and feedback on this work.

I would like to thank all the people that contributed to this work from the inspiration to realization. I would like to thank in the first place Yves Drolet for his work and dedication to our group by the help and joy he provides to us, in and out the laboratory.

I thank my former and present colleagues and friends who supported and advised me during this amazing adventure: Anthony, Joaquin, Manuel, Yasser, Lariel, Luan, Fabio, Dieudonné, Alexandre, Zhaojing, Ramon, Ramin, Molood, Shahid, Hamza, Shin, Melchiade, Youssef, Prajwal, Omar, Orlando, and Tian. Thank you for your help and time during this one-year project, I learned a lot and hope that I will be able to continue by your side.

Many thanks to Flavia Visentin for the amazing work she is doing, especially with Create Seed.

I thank Cornelia Chilian, Darren Hall and all the Slowpoke team working at Polytechnique for their precious time, advice, and contribution to this study.

I thank Lyne Dénommé for her work through the administrative process and kindness with which she helped me.

I thank the whole team of ICI, Mirko, Fyrial, Chuan Yi and Mike for their help and expertise.

I thank Denis Rho for the precious exchange on experiences we shared.

I thank Professor Clara Santato for the chance, support, and inspiration she gave me to be part of this team and work on this project.

I would like to thank Pagora and my professors for this international opportunity and their help. I thank Professor Anne Blayo and Professor Nathalie Marlin for their support and kindness through this experience.

RÉSUMÉ

Mots clés: *Biopigment, électronique organique imprimée, développement durable, encre biosourcée, Sépia melanine*.

Les matériaux électroniques organiques représentent un intérêt pour le développement de technologies durables dans les domaines de l'électronique et du stockage électrochimique d'énergie. Les déchets liés aux équipements électroniques et électriques, par leur accumulation, peuvent engendrer des effets toxiques sur la santé et l'environnement. L'impression de matériaux électroniques organiques sur papier se révèle être une alternative compostable, permettant de réduire ces déchets.

La Sépia mélanine est une des formes naturelles de l'eumélanine, un pigment foncé (noir-marron), pouvant être extrait à partir de l'encre de seiche (*Sepia Officinalis*). Ce pigment est abondant par sa présence au sein de beaucoup d'espèces vivantes, en particulier pour les fonctions biologiques qu'elle apporte. La Sépia mélanine est principalement constituée d'unités monomériques telles que des groupes fonctionnels d'indoles. Après plusieurs étapes de polymérisation et d'arrangement structurel de ces unités, des granules de taille nanométrique peuvent être formées. Récemment, l'impression de fines couches d'encres à base de Sépia mélanine ont permis de démontrer la prédominance d'un transport de porteurs de charge de type électronique dans ce pigment. Ce qui est inusuel pour de matériaux d'origine biologique dont le type de transport est souvent ionique.

Ce travail implique l'étude de l'imprimabilité sur support papier *Kromekote*®, ainsi que des réponses électriques d'encres à base de Sépia mélanine. Le support papier est pré-imprimé par flexographie avec un motif d'électrode dont la distance inter-électrode est de l'ordre d'une centaine de micromètres. L'étude de l'imprimabilité des encres à base de Sépia mélanine repose sur des tests rhéologiques et de mouillabilité. Les réponses électriques, quant à elles, sont obtenues à partir de mesures potentiostatiques (courant-temps à voltage constant, I-t) et de caractéristiques courant-potentiel (I-V) conduites entre 0 et 10 V à différentes vitesses de balayage du voltage de 1 à 500 mV/s. L'influence de l'humidité sur la réponse électrique est étudiée au travers de ces mêmes mesures électriques dans différentes conditions atmosphériques (azote sec, air ambiant et air humide). Les premiers résultats témoignent d'une conductivité des dispositifs prometteuse, offrant des opportunités pour une électronique plus respectueuse de l'environnement.

ABSTRACT

Key words: *Bio-pigment, printed organic electronics, sustainability, bio-sourced ink, Sepia melanin*.

Natural organic materials are keys for the eco-design of electronic devices and their powering elements (batteries). Printing natural organic materials on paper paves the way for composting electronic devices. This enables to alleviate the accumulation of Electrical and Electronic Equipment Waste (E-waste) whose effects on human health and the environment are harmful.

Sepia melanin is one of the natural forms of eumelanin, a black-brown bio-pigment of the melanin family. Melanin bio-pigments are ubiquitous in nature; they are key to diverse bio-functions in fauna and flora. Sepia melanin is extracted from cuttlefish (i.e. *Sepia Officinalis*) ink. It is mainly constituted of indole-based monomers. After several steps of hierarchical development, Sepia melanin building blocks feature nanometric granular structure. Recently, printed films including Sepia melanin showed predominant electronic transport.

This work focuses on the printability of films of Sepia melanin-based ink on *Kromekote*® paper and their electrical response. Paper substrates are pre-patterned by flexographic printing featuring electrode pairs with an interelectrode distance of about 100 µm. Ink printability study on paper relies on ink rheology and wettability tests. The electrical response is obtained from potentiostatic (I-t at constant voltage) and current-voltage (I-V) characteristics for applied electrical biases ranging between 0.1 V and 10 V and different voltage sweeping rates (1 - 500 mV/s. Humidity's influence on the electrical response is studied through these same electrical measurement protocols in different controlled conditions (dry nitrogen, wet air and ambient air). Preliminary results show a remarkable electrical conductivity of the films, paving the way towards more sustainable electronic devices.

TABLE OF CONTENTS

LIST OF TABLES

LIST OF FIGURES

LIST OF SYMBOLS AND ABBREVIATIONS

A	Area
AFM	Atomic Force Microscopy
cos	Cosinus
Dct/TRP2	Enzyme Dopachrome Tautomerase
DHI	5,6-dihydroxyindole
DHICA	5,6-dihydroxyindole-2-carboxylic acid
SDGs	Sustainable Development Goals
t	Thickness
E-waste	Electrical and Electronic Equipment Waste
G	Grammage
HOMO	Highest Occupied Molecular Orbital
I	Current
ICP	Inductively Coupled Plasma Spectrometry
L	Interelectrode distance
l	Length of the electrode
LUMO	Lowest Unoccupied Molecular Orbital
m	Mass
m_1	Mass 1
m_2	Mass 2
NAA	Neutron Activation Analysis
OFET	Organic Field-Effect Transistor
OLED	Organic Light-Emitting Diode

PVB	Polyvinyl Butyral B-30HH
R	Electrical resistivity
S	Surface
SEM	Scanning Electron Microscopy
S_r	Ring Surface
t	Time
U	Potential (Voltage)
V	Voltage (Potential)
V	Volume
W	Width
γ_{LG}	Interfacial tensions liquid-gas
γ_{SG}	Interfacial tensions gas-solid
γ_{SL}	Interfacial tensions liquid-solid
θ_0	Contact angle at equilibrium
ρ	Volumetric mass
σ	Electrical conductivity

LIST OF APPENDICES

CHAPTER 1 INTRODUCTION

1.1 Sustainability

In November 2022, the world's population reached an important stage of 8 billion people. Since the nineteenth century, an exponential tendency is observed concerning the world's population growth. It was estimated to be 2.5 billion people around 1950 and is expected to reach more than 10 billion in 2080 [1]. Demographic milestones also come through economic changes, notably the consequences of industrial revolutions that started to occur in 1780 with the industrialization in England, and later continued with the globalization in 1960 [2]. With it, the raise of environmental awareness lays the foundations for work and studies on the anthropogenic impacts on our planet. Indeed, in 1962, Rachel Carson published Silent Spring, referring metaphorically to the birds dying due to a massive pesticides and irrigation use in the United States, after World War II, during the Third Agricultural (Green) Revolution [3]. This awakening led to many debates and ideologies from the most pessimist theory in which the growth model should be abandoned, to the most optimistic where natural cycles should be human-made and regulated thanks to, for instance, geo-engineering.

In this context, the notion of Sustainability saw the light of the day with the Brundtland Report in 1987 with the World Commission on Environment and Development by the United Nations. Sustainable development was defined as follows: "meeting the needs of the present without compromising the ability of future generations to meet their own needs" [4]. However, as our societies are constantly evolving, many questions have been raised about the definition of needs both present and future. Indeed, development is an anthropocentric notion which does not have the same meaning for all. Depending on the region of the world, the needs are different. Even more complex is the identification of the needs for the future generations because of uncertainty and the cruciality of anticipation of future life standards and technologies, without yet knowing it. These questions led to different degrees of definitions of sustainability, depending on the point of view, and the importance granted to environment, social, and economic development, as it constitutes a multi-criteria notion. Three main categories of sustainability emerged: weak, strong, and very strong which are mainly distinguished by the identification of human well-being. In the weak

sustainability anthropocentric vision, human well-being is conferred by possessions or services maintained through time, and so every resource can be converted into a capital if it satisfies this condition. For the very strong eco-centric vision, every resource or capital is unique and so, cannot be converted, it should be conserved the way it is. However, it is too restrictive for human being. In a strong vision, resources and capitals can be converted while critical resources are not at stake and can be preserved at a certain point. The exploitation rate should not exceed the renewing rate or the adaptation rate to other technologies in the case of unrenewable resources. The main issue with this vision is the anticipation of future generations needs and so the definition of which resources are critical or not [5].

That is why, in 2015, the Division for Sustainable Development Goals (SDGs) was created by the United Nations bringing forward 17 SDGs to attempt sustainable development for our society. This agenda was elaborated after several summits about sustainability, that began in 1992 with the Earth Summit in Rio de Janeiro, followed by others that helped to enrich the vision of sustainability and how it can be defined and achieved. These goals emphasize as much social, as economic, and as environmental aspects and their challenges. Among these we can cite: no poverty and hunger (G1&2), quality education (G4), decent work and economic growth (G8), responsible consumption and production (G12) and peace, justice, and strong institutions (G16) [6].

In this sense, to reach a sustainable development in our society, it is crucial to have a global awareness and so consider ethics in our everyday lives and work. The aspects that were given prominence in this section, establish the context, broad motivation and potential impact for the work presented in this dissertation.

1.2 Printed organic electronics

The exponential growth population and the dependence on electronics have induced a massive consumption of electronic devices, leading to the accumulation of 53.6 Mt of E-Waste (Electrical and Electronic Equipment Waste) in 2019, as reported by the United Nations [7]. In 2030, the global E-Waste is estimated to reach 74.7 Mt. It was keeping these numbers in sight that the idea of exploiting printed organic electronics to create low cost, high manufacturing capability and compostable devices, emerged. In this sense, printed organic electronics can become a key to several issues at stake such as E-Waste and the use of *critical* elements. Indeed, for some specific

applications, organic electronics can substitute inorganic (conventional) electronics which often require the use of critical elements. Further, organic materials complement conventional inorganic electronic materials and as such allows a diversification in the electronics sector [8].

Organic electronics are based on polymers or small molecules mainly composed of carbon and that feature properties of electrical conductivity. This is made possible thanks to electronic *conjugation* in their molecular structure that permit electronic delocalization [9]. The first record of organic material conduction occurred in 1963 when R. McNeill and coauthors showed the conduction of polypyrrole doped with iodine. Indeed, pyrolysis of tetraiodopyrrole can lead to the presence of iodine in the polymer structure. The resistivity of polypyrrole (organic semiconductor) is between 1 and 200 Ohm.cm (corresponding to an electrical conductivity between $1\,S.cm^{-1}$ and $5 \times 10^{-3}\,S.cm^{-1}$) [10].

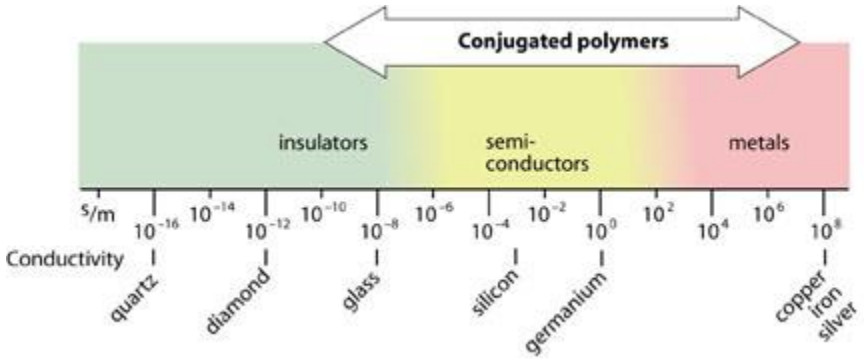

Figure 1.1 Conductivity ranges of insulators, semiconductors and metals. Adapted from [11]

The study of organic materials for electronics went further from 1976 and later on with the Nobel Prize in Chemistry awarded in 2000 to Heeger, MacDiarmid and Shirakawa for the discovery of organic conducting polymers (polyacetylene, polyaniline), chemically doped [12]. Since then, many polymers were studied for their electrical properties that can be suited for electronic devices, such as poly(3-hexylthiophene), poly(9,9′-dioctylfluoreneco-benzothiadiazole) or polydopamine [13], [14]. Coupled with printing techniques, organic electronics can be developed with flexible substrates, representing an interest for biomedical sensors adaptable to human body shapes and skin. Recently, A. Camus et al. used the bio-pigment Sepia melanin (a poly-indole-like material)

as potential candidate for greener printed organic electronics. Sepia melanin films showed a conductivity of $10^{-3}\ S.cm^{-1}$ [8].

Recently, life cycle analyses aiming at providing metrics on the environmental impact of different approaches to electronic products have been proposed. For instance, A. Sudheshwar et al. [15] investigated the climate change impact of printed circuit boards (PCBs) made with flame retardant (FR4) and printed electronics on paper substrates through a life cycle analysis (LCA). They reported a lower impact (climate change in kg CO_2 eq.) of printed electronics substrate materials compared to the PCB counterparts (Figure 1.2). However, they estimated higher impact on climate change for printed electronics regarding the conductive materials compared to the ones used in the fabrication of PCB (Figure 1.3). This brings about the importance of developing more sustainable conductive inks and materials for printed electronics on paper. More research is expected in the years to come in the field life cycle analysis in the electronics sector, to quantitatively evaluate the economic, environmental, and societal impact of conventional in opposition to greener approaches.

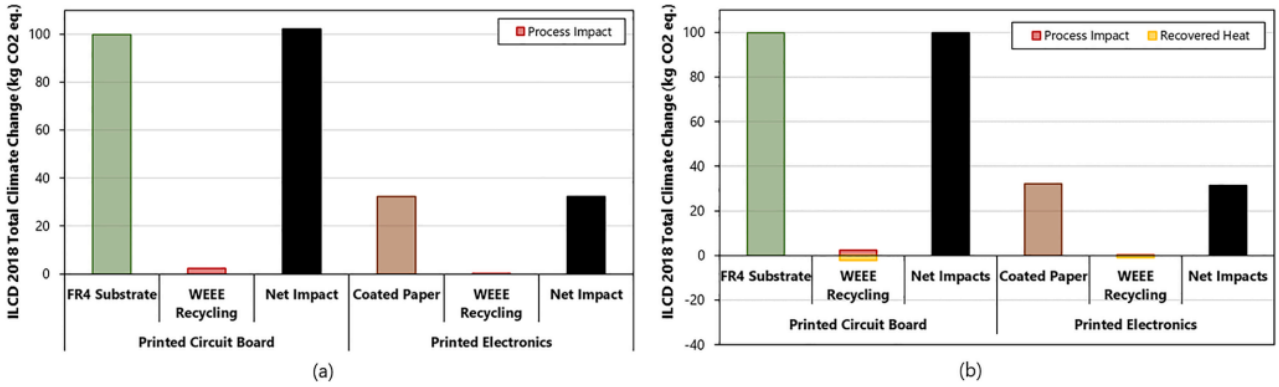

Figure 1.2 Life cycle analysis focused on climate change impact, represented as “Net impacts” comparing the substrate materials of printed circuit boards and printed electronics in two different scenarios, with and without recycling benefits. Adapted from [15]

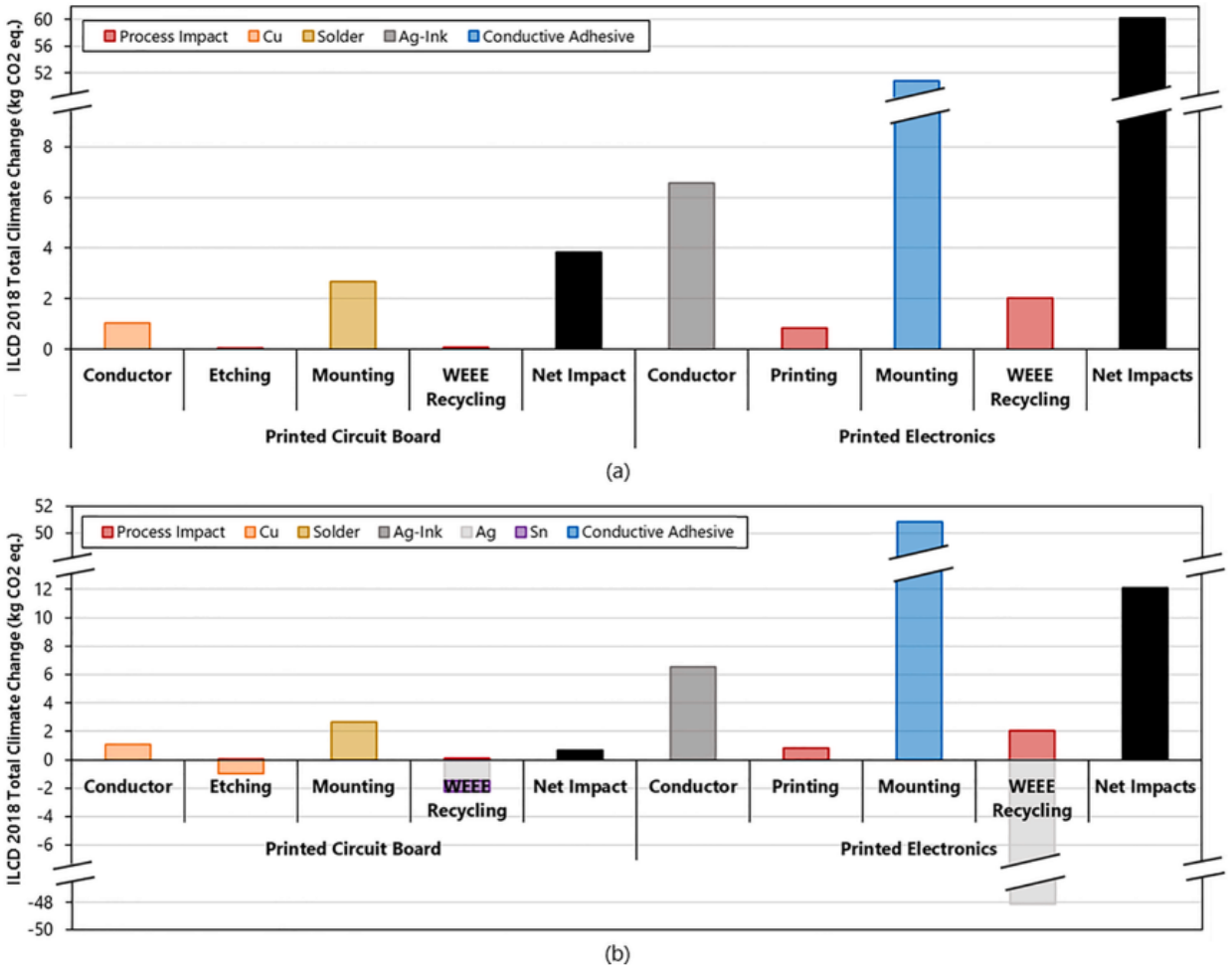

Figure 1.3 Life cycle analysis focused on climate change impact, represented as "Net impacts" comparing the conductive materials of printed circuit board and printed electronics in two different scenari with and without recycling benefits. Adapted from [15]

1.3 Research objectives

This work aims at humbly contributing to design and develop sustainable processes, technologies, and electronic and electrochemical organic devices. It deals with the study of bio-sourced materials and their processing to assess their potential for biodegradable organic electronics. The study is centered on two main aspects: the former is the processing of this bio-pigment into an ink and the physicochemical characterization of the printed films; the latter is the exploration of the electrical response of the films obtained from the Sepia melanin-based printable inks.

Many challenges are associated to this study, particularly related to the intrinsic properties of Sepia melanin. Indeed, the heterogeneous chemical composition of the *biosynthesized* Sepia melanin entails complexity to determine, among other aspects, the effect of the presence of metallic chemical elements on the electrical response. Sepia melanin is poorly soluble in common organic solvents. In this sense, binders are used for Sepia melanin-based ink formulation. The use of additional materials to fabricate films leads to even more difficulties characterizing the electrical properties of Sepia melanin. According to the aspects just discussed, the objectives of this research project are the following:

Studying the printability of the formulated inks' and the printed films' properties

The characterization of the printed films and the paper substrates is key to study the film-electrode interface. This is essential to assess potential applications of the material. This characterization also brings information that can help to design pre-treatments to enhance device biodegradation at the device's end-of-life.

From an experimental point of view, the study of the ink printability will be carried out through rheologic tests. Paper substrates will be investigated for their weight and dimensions (grammage and thickness), water absorption (Cobb Test) and contact angle (tensiometer). The same characterization will be held for the printed substrates, including those that undergone a post-printing treatment (e.g. thermal treatment for binder and Sepia melanin cross-linking). The morphological characterization of the printed films was realized through Scanning Electron Microscopy (SEM), with and without thermal treatment.

Studying the electrical response of Sepia melanin-based samples

Current-voltage (I-V) and potentiostatic (current-time (I-t) at a fixed voltage) measurements were conducted for the characterization of the electrical behavior of the Sepia melanin-based films. Carrying out these measurements in different atmospheric and thermal conditions permit to evaluate the potential for device applications as humidity and temperature sensors.

Determination of the chemical composition of the samples

The investigation of the chemical composition aims at determining qualitatively and quantitatively the presence of metallic chemical elements in the Sepia melanin-based inks. It is worth noticing that metallic elements could affect the electrical response of the samples. Neutron Activation Analysis (NAA) is an ideal technique that could be complemented with Inductively Coupled Plasma Spectroscopy (ICP).

The measurements operated in this MSc project are listed in Table 1.1.

1.4 Structure of the dissertation

Chapter 1 is an overview of the fundamentals and challenges of this study and the objectives related to them. It also provides the structure of the dissertation.

Chapter 2 is a literature review of eumelanin, the bio-pigment of interest in this project. The aim of this literature review is to describe the material considered in this project, which is key for the interpretation of the experimental results.

Chapter 3 focuses on experimental methods, from the extraction of the Sepia melanin from the Sepia (cuttlefish) ink to samples' characterization.

Chapter 4 presents the results and discussion about inks, substrates, and printed samples. A part revolves around the electrical characterization of the printed films (with and without thermal treatment) and bare paper substrates. It also proposes possible routes for more sustainable inks, to minimize the use of chemicals during the ink formulation.

Chapter 5 includes conclusion and possible future experiments for this project, e.g. mechanical and physicochemical tests to better understand printed film/electrode and printed film/substrate interfaces, aiming to enhance biodegradation through mechanochemistry.

Table 1.1 Synoptic table of the measurements carried out in this MSc project.

	Name			**Extracted Sepia melanin**	**Sepia-shellac ink**		**Commercial Sepia ink**	**Natural Sepia ink**
	Type			Powder	Ink		Ink	Ink
	Source			Chemically-extracted powder from commercial Sepia ink	Formulated from extracted Sepia melanin, shellac (binder) and 1-propanol (solvent)		Ink processed by food-processing industry from natural Sepia ink (edible NaCl added)	Hand-extracted from cuttlefish ink sack (raw)
	Specie			*Sepia Officinalis*				
	Type of measurements	***Atmosphere***	***Type of substrates***	**Extracted Sepia melanin**	**Non-cross-linked Sepia-shellac**	**Cross-linked Sepia-shellac (thermal treatment)**	**Commercial Sepia ink**	**Natural Sepia ink**
Elemental composition	**Neutron Activation Analysis (*NAA*)**	/	*Neutron Activation Analysis (NAA)*	**1**	**1**	0	**1**	**1**
Printability and hydrophobicity	**Viscosity**	*Ambient*	*Viscosity*	0	**3**	0	**3**	0
	Contact angle	*Ambient*	*Ink drop on paper substrate*	0	**1**	0	**1**	0
			Ink drop on spin coated on SiO_2	0	**1**	0	**1**	0
			Water drop on ink film	0	**1**	0	**1**	0
Films weight, dimensions and water absorption	**Grammage**	*Ambient*	*Printed on paper substrate*	0	**6**	**6**	0	0
	Thickness	*Ambient*	*Printed on paper substrate*	0	**6**	**6**	0	0
			Ink drop on spin coated on SiO_2	0	0	0	**5**	**1**
	Cobb Test	*Ambient*	*Printed on paper substrate*	0	**6**	**6**	0	0
Imaging	**Scanning Electron Microscopy (*SEM*)**	*Ambient*	*Spin coated on SiO_2*	0	0	0	**1**	0
			Printed on paper substrate (ESEM)	0	**1**	0	0	0
Films electrical response	**Current-Voltage characteristics (I-V)**	*Ambient*	*Printed on paper substrate*	0	**6**	**2**	0	0
		Ambient	*Spin coated on SiO_2*	0	0	0	**1**	**1**
		Dry N2, ambient, and humid	*Spin coated on SiO_2*	0	0	0	**5**	0
	Potentiostatic characteristics (I-t)	*Ambient*	*Spin coated on SiO_2*	0	0	0	**1**	**1**

CHAPTER 2 LITERATURE REVIEW

2.1 Printed organic electronics

2.1.1 Organic electronics

Organic semiconductors, compared to inorganic ones, feature lower charge carrier mobility (drift speed per unit of electric field). Nevertheless, they offer advantages permitting less complex (solution-based deposition, at room temperature and ambient pressure) and costly fabrication protocols, with respect to their inorganic counterparts. Further, they provide chemical *tailorability* of their molecular structure through organic chemical synthesis. Such *tailorability* translates into the versatility of the functional properties e.g. for the color of the light they can emit (exploited in organic light-emitting diodes (OLEDs)). [16]–[18]. Organic semiconductors, for their softness, are relevant for conformable (flexible) (bio)electronics.

Despite many organic materials being insulating by nature, some of them, with specific molecular structures, allow charge carrier delocalization and transport. These specific molecular structures feature conjugation. Conjugated molecular materials, by alternation of simple (sigma, σ) and double (pi, π) bonds, permit electronic delocalization. Charge carriers can move within delocalized molecular orbitals bringing about transport.

A well investigated class of organic electronic devices is that of transistors, which are devices acting as current switches and amplifiers. Transistors make use of semiconductors, and their working principle is based on doping. Doping aims at controlling the density of charge carriers in a semiconductor. Electrons are the charge carriers in metals whereas both electrons and holes can be the charge carriers in semiconductors. N-type doping induces an increase in electron density. P-type doping results in the increase in hole density [21], [22].

If metals have conductivities of about $10^5\ S.cm^{-1}$, semiconductors have conductivities in the range of $10^{-8}\ S.cm^{-1}$ to $10^2\ S.cm^{-1}$ [19], [20].

Several device structures are possible for transistors. One type of transistor device structure is the top gate, bottom source and drain structure, illustrated in Figure 2.1. It can be described as follows: source and drain electrodes patterned on a substrate define the transistor channel where the semiconductor is deposited. The dielectric is located on the semiconductor and, on top of the

dielectric, can be located the gate electrode. When a source-drain voltage is applied (V_{DS}), a drain-source current flows in the channel (I_{DS}) and its value is controlled by the gate-source voltage (V_{GS}) [21].

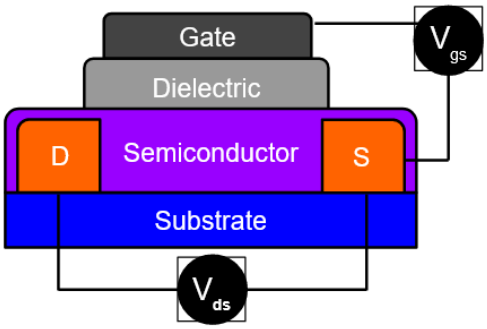

Figure 2.1 Scheme of top-gated, bottom source and drain transistor structure.

2.1.2 Printing technologies for electronics

Printing technologies provide possible versatile design and less expensive manufacturing for devices on a wide range of substrates. It also brings major assets when it comes to mechanical and optical properties, permitting to achieve flexibility and different degrees of optical transparency or opacity.

Nevertheless, printing can be limiting due to the maximum spatial resolution, comprised between 100 and 10 µm for gravure, flexographic, inkjet and screen printing. As a comparison, the usual patterning technique for microelectronics, i.e., photolithography, has resolutions between 10 to 1 µm. The resolution affects the minimal possible interelectrode distance [16].

The substrate also plays an important role as metallic patterned electrodes are usually patterned on SiO_2, which has a smoother surface than paper or plastics typically used in printing technologies.

Due to the natural porosity of paper, many techniques were developed such as calendaring and surface coating to diminish paper roughness. Indeed, paper surface porosity can entail printing defects and potential surface contamination with undesirable particles within the pores. Calendared paper consists in compressing the paper between two rolls to mechanically press the pores. Suspensions used for coating usually contain fillers and particles, such as titanium dioxide, kaolin

(aluminum silicate clay) or calcium carbonate clay to fill the pores. Coating can also bring paper surface functionalization to enhance ink wettability [22].

Yet, there are still challenges related to ink formulation for printing technologies, depending on the technique used. For instance, the ink viscosity can be tailored to ensure proper adhesion to the substrate surface or avoid deep ink absorption. For flexographic printing, the viscosity range is usually between 0.01 and 0.1 Pa.s, to obtain a resolution of 60 lines per cm [23].

The formulation of conducting inks where transport is percolative, requires attention to the conductive material and binder ratio to find a balance for proper dispersion and homogeneity, which are provided by the binder. This aspect has been studied in our group through printed electronic devices with Sepia melanin-based ink including polyvinyl butyral B-30HH as binder [8]. We found that the optimal ratio to obtain high electrical conductivity was beyond 40-50 wt% of Sepia melanin. Indeed, by increasing the concentration of Sepia melanin, which is the conductive material, the distance between Sepia melanin granules diminishes, creating percolation paths for conductivity.

Recent works also highlight bio-sourced materials that can be used as binders in ink formulation such as shellac resin. Shellac is a polymer resin made by the excretion of tree sap from specific insect (*Laccifer lacca*), mostly located in South-East Asia. Shellac features hydrophilic and hydrophobic functions in the molecular structure as shown on Figure 2.2. This amphiphilicity (simultaneous hydrophobicity and hydrophilicity) constitutes an interesting asset for the dispersion capability of shellac when used as binder [24], [25].

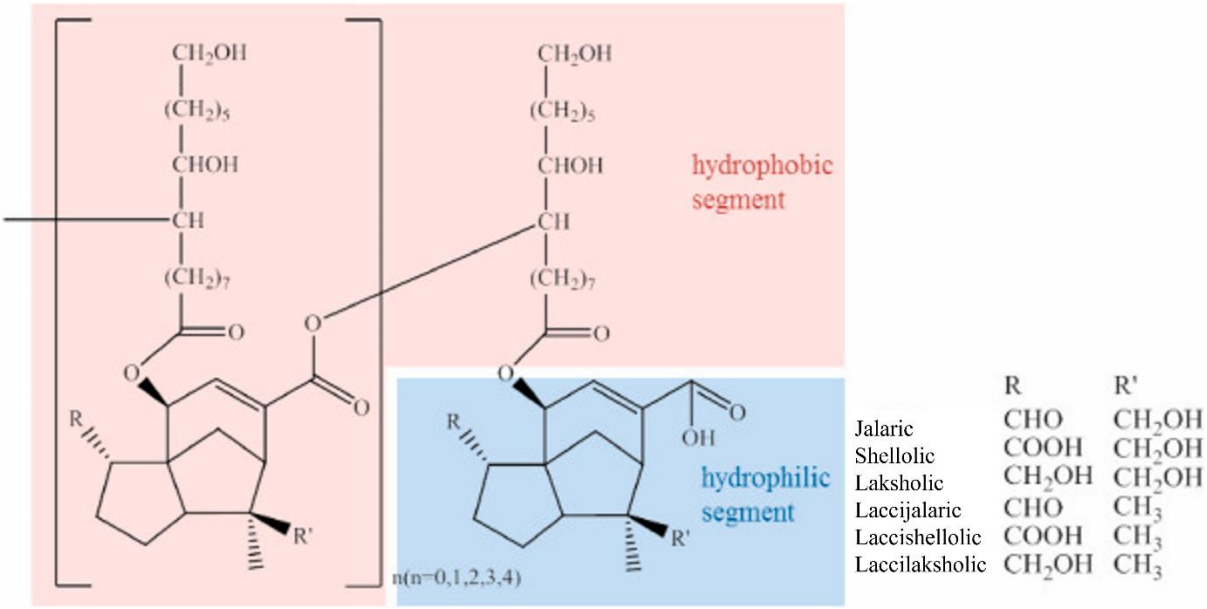

Figure 2.2 Molecular structure of shellac showing amphiphilicity. Adapted from [25].

Shellac is usually extracted and *bleached* using sodium hypochlorite (NaClO) or hydrogen peroxide (H_2O_2).

Shellac features key thermal properties as its softening and melting temperatures are very close: between 65 and 70 °C for softening and 75 to 80 °C for melting. After melting, cooled shellac can become rigid and fragile, forming a flake-like resin [24]. Indeed, shellac features physical cross-linking below 70 °C by forming weak interactions such as H-bonding or van der Waals. However, beyond 70 °C, it features a chemical cross-linking by forming covalent bonds through an inter-esterification between hydroxyl and carboxyl groups.

2.2 Eumelanin

2.2.1 Fundamentals

Organic materials that feature electrical properties and obtained from natural sources (bio-sourced), by involving less organic chemical synthesis steps, can find potential applications for electronic devices. This is the case of melanin bio-pigments.

Melanins are the most abundant family of bio-pigment on Earth, present both in fauna and flora. Allomelanin, a member of the melanin family, is present in plants and fungi. Pyomelanin in micro-organisms such as bacteria. Neuromelanin in certain locations of the human brain. Pheomelanin (red-yellow pigment) and eumelanin (black-brown pigment) are present in animal skin, hair and eyes [26], [27].

The eumelanin pigment is known to have a protective action against ultraviolet radiation, thus reducing the probability of developing skin tumors and cancers.

Eumelanin can be produced to color skin, feather, fur, or scale with a certain motif for stealth such as felines, reptiles, and birds. Another example is for marine animals, especially cephalopods for which eumelanin based inks are synthetized to be released as a defensive tool that blind predators [26]–[29].

This study focuses on eumelanin from *Sepia Officinalis*, a cephalopod species known as cuttlefish. The eumelanin from *Sepia Officinalis* is more commonly referred as Sepia melanin. The cuttlefish produces naturally the eumelanin, which is stored in an organ called *ink sack*. From this organ, the Sepia melanin ink can be expulsed in case of danger or threat to muddle predators thus permitting to cuttlefishes to flee without being seen. Being edible, cuttlefish ink obtained from the ink sac becomes then a food-processing industrial *byproduct*, and can therefore be used for diverse purposes [29].

2.2.2 Molecular structure

Eumelanin is based on functionalized indole groups, i.e.: 5,6-dihydroxyindole (DHI) and 5,6-dihydroxyindole-2-carboxylic acid (DHICA) (Figure 2.3). DHI and DHICA are present in different ratios, which is usually between 10 to 50 % of DHICA, depending on the synthesis conditions [28].

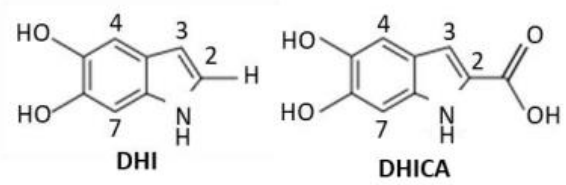

Figure 2.3 Molecular structures of 5,6-dihydroxyindole (DHI) and 5,6-dihydroxyindole-2-carboxylic acid (DHICA). Adapted from [28].

The synthesis of eumelanin, and in particular Sepia melanin, as for all biosynthesized natural materials, is influenced by factors such as the synthesis environment, geographic location, season of the year etc. In this sense, the exact mechanism of the Sepia melanin's synthesis and its structure is still not exactly determined. Several models available in the literature describe the formation process and structure of eumelanin. Such models are based on Scanning Electron Microscopy (SEM), Transmission Electron Microscopy (TEM) and Atomic Force Microscopy (AFM) observations [30], [31], [27], [32].

There are common aspects in the available models. The most important aspect is the *hierarchical* development of the material. Firstly, DHI and DHICA building blocks undergo an oxidative polymerization to form oligomers from about 4-6 monomer units. The polymerization can occur at different locations in the DHI and DHICA molecules, mainly on sites 2, 3, 4 and 7, except for DHICA where the site 2 is unavailable due to the presence of the carboxyl group. The fact that several sites can participate to the formation of chemical bonds leads to chemical disorder in the melanin macromolecule (chemical heterogeneity) [28].

Being planar and electronically conjugated, the DHI and DHICA monomers can form planar oligomers that, in turn, can form nanoaggregates (protomolecules) by π-π stacking (non-covalent bonding) with a typical interplanar distance of about 3.4 Å and about 10 to 20 Å high. Such nanoaggregates can further stack through π-π stacking and edge-to-edge H-bonding, to form structures from 4 to 15 nm-high and 20 nm-long. These structures aggregate to form the 100-200 nm-sized granules typical of Sepia melanin (Figure 2.4) [28]–[34].

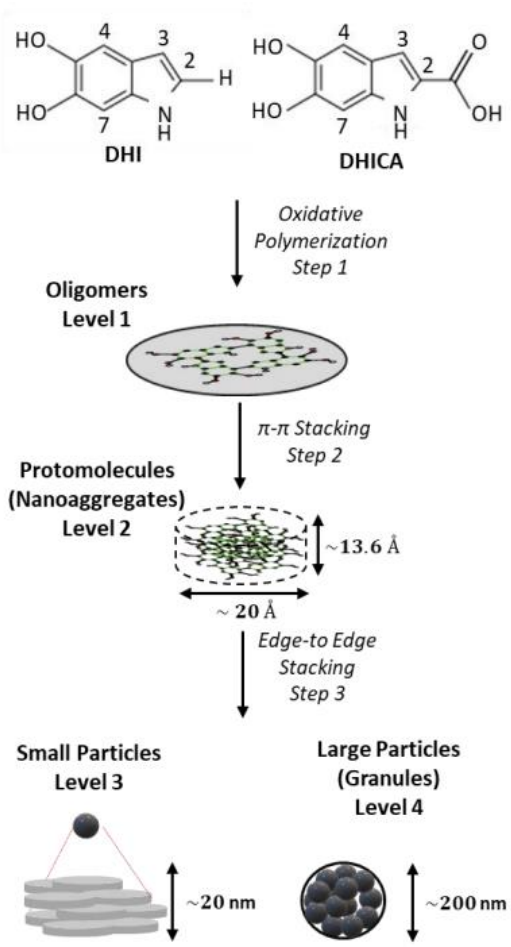

Figure 2.4 Process of hierarchical formation of Sepia melanin, from monomers to granules. Adapted from [28].

The chemical synthesis of eumelanin, called melanogenesis starts from L-tyrosine ((2*S*)-2-amino-3-(4-hydroxyphenyl) propanoic acid), an amino acid. Tyrosine is oxidized into dopaquinone. Dopaquinone can be cyclized into cyclodopa that through redox processes with dopaquinone can form L-dopa (L-3,4-dihydroxyphenylalanine) and dopachrome ((2*S*)-5,6-dioxo-2,3-dihydro-1*H*-indole-2-carboxylic acid). Afterwards, in presence of the enzyme dopachrome tautomerase (Tyrp2), dopachrome can be tautomerized to form DHICA. Tautomerization is a change of chemical structure (isomer) by protonation or/and double or triple bond delocalization via an internal reaction. In absence of this enzyme, dopachrome can be turned into DHI by liberation of carbon dioxide (CO_2) (Figure 2.5) [27], [31], [32].

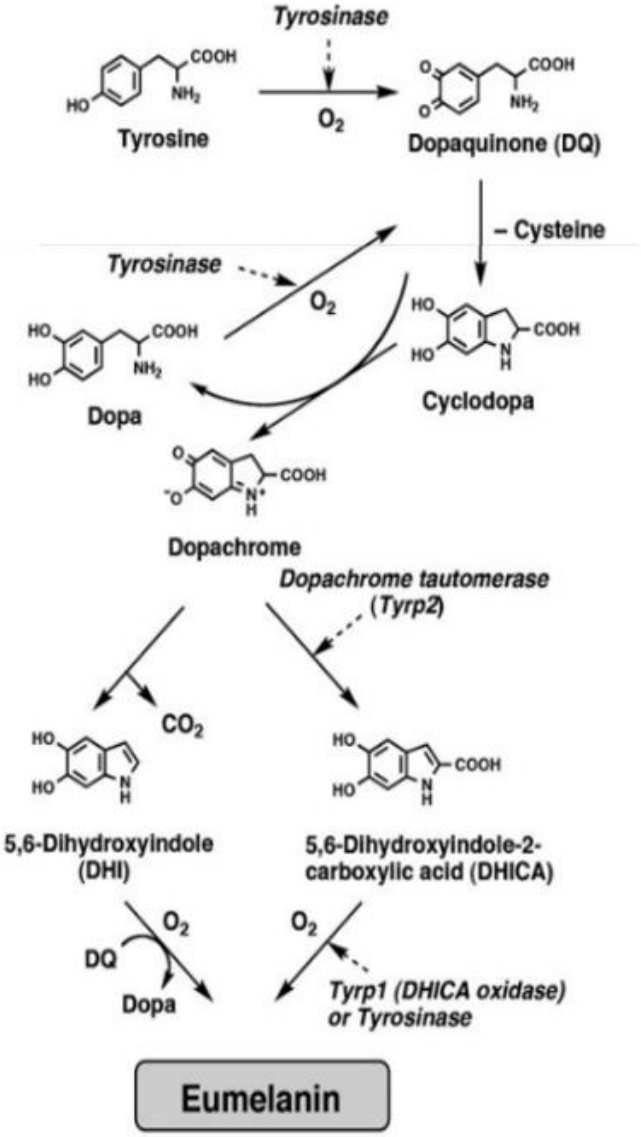

Figure 2.5 Synthesis steps of DHI and DHICA building blocks and eumelanin obtained from them. Adapted from [28].

The extraction of eumelanin from Sepia Officinalis' ink is challenging since the biopigment is poorly soluble in water and common organic solvents, due to its chemical disorder. Eumelanin extraction is typically carried out in acidic environments, where the pigment can be precipitated [29].

The biodegradation of eumelanin in industrial compost conditions (following the ASTM D5338 standard) has been reported in [33]. It was observed that after 98 days in industrial compost (58 °C with humidity control) the mineralization rate of Sepia melanin was around 37 %. The mineralization rate is the amount of the CO_2 released by the test sample with the subtracted amount of CO_2 of the blank compost (reference) over the total amount of released CO_2.

2.2.3 Electrical properties

One of the first studies on the electrical properties of eumelanin was led by J. McGinness [35] who studied the conductivity of eumelanin hydrated pellets. The electrical measurements of these pellets show a reversible switch behavior with an increase of the current of one order of magnitude from a threshold voltage as shown on Figure 2.6. The thickness of the pellets (0.1, 1 and 10 mm) influences the threshold voltage for the electrical switch.

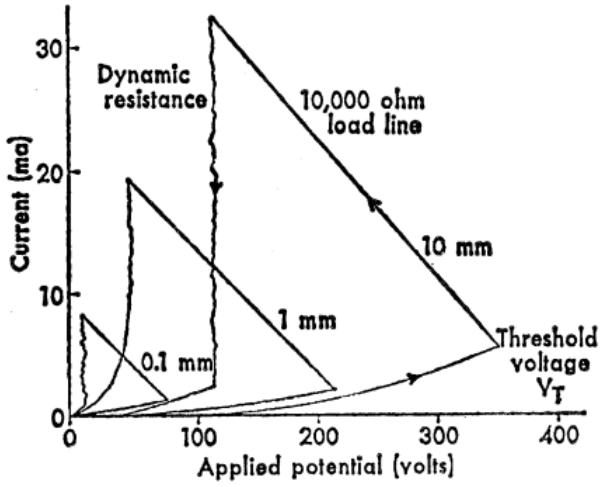

Figure 2.6 Current-voltage (I-V) characteristics of hydrated eumelanin pellets with different thicknesses. Adapted from [35].

Mostert et al. [36] proposed the hypothesis of mixed electronic and ionic conduction in Sepia melanin. They considered that DHI and DHICA can feature at ambient conditions different redox forms: oxidized (quinone form), intermediate (semiquinone) and reduce (hydroquinone) forms. [28], [29], [32]. In presence of water, there is a *comproportionation* reaction between the reduced and the oxidized forms towards the intermediate form with liberation of protons. The semiquinone

form includes an intrinsic spin radical considered by Mostert et al. the electronic charge carrier produced together with a proton in the *comproportionation* reaction (Figure 2.7).

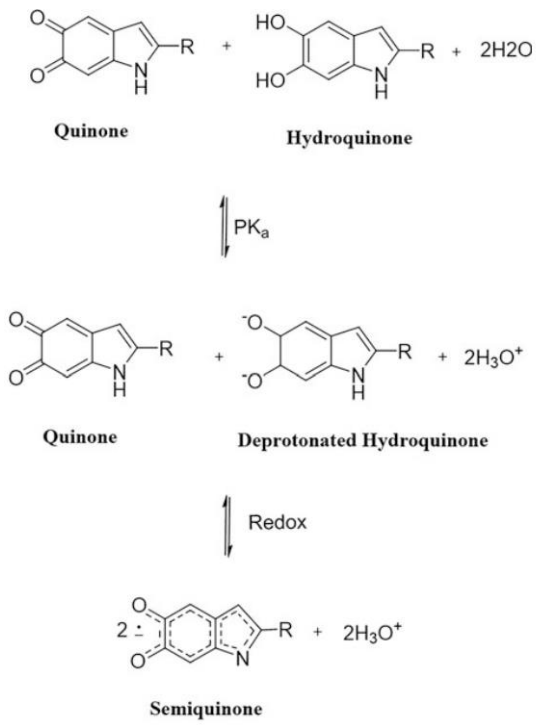

Figure 2.7 Comproportionation reaction in presence of water between oxidized (Quinone) and reduced (Hydroquinone) forms of the building blocks of eumelanin (DHI or DHICA); the products of the reactions are electronic (extrinsic radical on the semiquinone) and ionic (protonic) charge carriers. Adapted from [29].

More recently, our group [8] investigated printed films from Sepia melanin ink formulated including polyvinyl butyral B-30HH as binder. The key observation is that films printed on paper or polyethylene terephthalate feature a conductivity of about $10^{-3}\ S.cm^{-1}$. Prior to this study, the highest conductivity reported for eumelanin was $10^{-4}\ S.cm^{-1}$ (in wet conditions) and $10^{-13}\ S.cm^{-1}$ (in dry conditions). The hypothesis they proposed is that the highest conductivity corresponds to an optimal concentration of Sepia melanin in the ink, i.e. a concentration that allows a inter-granule percolation path for the charge carrier [8]. Sepia melanin constitutes a unique bio-sourced material in terms of electrical properties due to its chemical structure, hierarchical build-up, and potential interface interactions with its environment (atmosphere, metal electrodes, electrolytes). Indeed, it is composed of conjugated oligomers, featuring hydroxyl and carboxyl

groups in their molecular structure, and that has a high affinity for metal ions opening the possibility to observe in the material electronic, protonic, and ionic (both cationic and anionic) transport [28], [37]. Its disordered structure (featuring physical heterogeneity) compared to other well-established organic semiconductors is the main factor leading to the challenging identification of the mechanisms explaining its electrical response. These aspects are still challenges remaining at stake.

CHAPTER 3 METHODOLOGY

3.1 Ink characterization and film fabrication

3.1.1 Sepia melanin extraction

The first step in the ink formulation is to extract the pigment, eumelanin, from *Sepia Officinalis* ink available as commercial ink, made by the food industry.

The commercial Sepia melanin ink used is from the *Stareef Seafood Boston* brand and contains cuttlefish ink and added salt with 14% of sodium, 10% of calcium and 1% of protein according to the Nutrition Facts table. The ink is recovered from the ink sack of the cuttlefish, the fishing area is the FAO 34, which corresponds to Eastern Central Atlantic: the Northern-West coast of Africa, from the Gibraltar's Detroit to the Congo's estuary.

Usually, the extraction requires 300 g of commercial Sepia melanin ink to obtain 30 g of Sepia melanin. The commercial Sepia melanin ink is conserved at low temperature (-3 °C). The extraction is made through several steps of centrifugation (*Allegra-X30R Centrifuge Beckman Coulter*) at 10000 rpm at 5 °C in different solvents: hydrochloric acid (500 ml 2M stirred at 400 rpm for 24 hours at room temperature), deionized water, ethanol, sodium phosphate (0.02% v/v of monobasic sodium phosphate 200 mM, 32.49 % v/v of dibasic sodium phosphate 200 mM and 67.49 % v/v of deionized water), and ethyl acetate. A powder is then obtained after lyophilization at -80 °C for at least three days (*Appendix A.2*) [38].

3.1.2 Ink formulation and rheology

Sepia melanin in the form of powder cannot easily give solutions; only suspensions of the powder can be prepared.

The use of a binder in the ink formulation is mandatory to have homogeneity and stability of the suspension. Dewaxed shellac (100 g), a bio-sourced resin, was used as binder, and 1-propanol (242 g) as solvent to reach a viscosity between 0,01 and 0,1 Pa.s, which is the usual range for flexographic inks. These two components are mixed in a high-rotation speed disperser (*1.5 hp, Engineered Mills Inc.*) at 500 rpm for 3 hours. After this first step, 100 g of extracted Sepia melanin

powder is added in the mixture at 350 rpm for 1 h. Afterwards, the ink is poured in an attritor (a high-rotation speed flat disc with 500 g of 1 mm-sized diameter zirconium oxide beads in a water-cooled vessel). The mixing step lasts 9 h at 2000 rpm with a total energy of 1.2 kWh; it allows to break agglomerates and promote the dispersion of Sepia melanin in the ink. The ink (22.62 w% of Sepia melanin) is then stored in a refrigerator at 5 °C, protected from light.

The ink viscosity is measured with an *Anton Paar MCR 92 ATS 5.0 Reologica instruments* rheometer. The viscosity is measured for 30 points with 5 sec between each point, to reach a total time of 150 sec, with a mechanical couple increasing from 0 mN.m to 14 mN.m.

3.1.3 Neutron Activation Analysis

The chemical composition of the different inks: natural, commercial, formulated Sepia-shellac, and extracted Sepia melanin powder, is essential to shed light on their functional properties. Neutron Activation Analysis (NAA) permits to identify elements present in a material and estimate their concentrations.

NAA relies on irradiation with neutrons the sample under study to form radioactive isotopes of the elements constituting the sample. The relaxation of the nuclei causes gamma-ray emissions such that the presence and amount of the elements can be determined from the absorption spectrum obtained. Since the excited nuclei emit gamma rays at an energy specific for each element, it is possible to perform an elemental identification.

Concerning the quantitative aspects, counting photons of one energy is related to the concentration of the element associated to such emission energy [39], [40]. The amount of one element is calculated by the area associated to the most intense photoelectric peak obtained at the corresponding energy.

To have a complete overview of the chemical composition of a material, the NAA technique can be complemented with Inductively Coupled Plasma (ICP) technique, as NAA usually allows the detection of elements with an atomic number higher than 9. This depends mainly on the half-life duration and the protocol of irradiation (*Appendix A.1*) [39], [40].

We characterized several inks by the NAA technique: natural and commercial Sepia ink, extracted Sepia melanin and Sepia-shellac formulated ink.

The NAA characterization was made at the *SLOWPOKE* nuclear reactor of Polytechnique using a combustible source of 5 kg of 20% U-235 enriched uranium. The first step was to weigh the sample with an analytic balance *Sartorius MSU 124-S* with a 0.1 mg precision, as the element concentration is expressed in ppm (µg mass of the element calculated / g mass of the weighted sample). The sample is then placed into a polyethylene vial and in the reactor for a 30 sec to 5h irradiation, depending on the half-life of the elements to be characterized, short or long. The thermal neutron flux applied is usually between $4.43 \times 10^{11}\ cm^2/s$ and $5.58 \times 10^{11}\ cm^2/s$. For the counting part, the gamma ray peaks were measured with a Ge gamma-ray detector *Ortec GEM55185* and the spectrum analyzed with *Multichannel analyzer Ortec DSPEC Pro*. The counting time varies for long and short half-life elements; as for the irradiation step, it can be around 15 min for short half-life to 10 hours for long-life ones, following the procedure in *Appendix A*. The accuracy of the amount related to the measured peak area is around 5% [39].

3.1.4 Ink deposition: flexographic printing and spin coating

After the elemental composition performed to characterize Sepia melanin extraction and the Sepia-shellac ink formulation efficiency, the ink can be used for printing. Our choice was made towards flexographic printing which is widely used, including with water-based inks. It is a cost-effective printing technique, allowing high production volume [23].

It requires a stencil in relief made of flexible photopolymer. Flexography is generally used for paper, cardboard, polymeric and metallic substrates. The printing is made thanks to the stencil in relief that transfers the pattern to print on the substrate. The stencil is thick enough to prevent the ink from entering the negative parts and induce printing defects. The stencil is fixed to a roll that is covered by ink only on positive part (relief). The ink is then applied to the substrate using a compression roll. The thickness of the ink-printed film is usually between 6 and 8 µm [16], [23].

The printing of the Sepia-shellac formulated ink on *Kromekote*® S1 paper is made with the laboratory-scale printer *RK Flexiproof 100,* using an anilox (cells: 15 billion cubic microns per square inch of surface, bcm). A doctor blade provides for the ink and regulated the amount deposited on the anilox. The ink is then transferred to the stencil (polymer printing plate) and the pattern is printed by the pressure applied on the substrate with the compression roll (Figure 3.1).

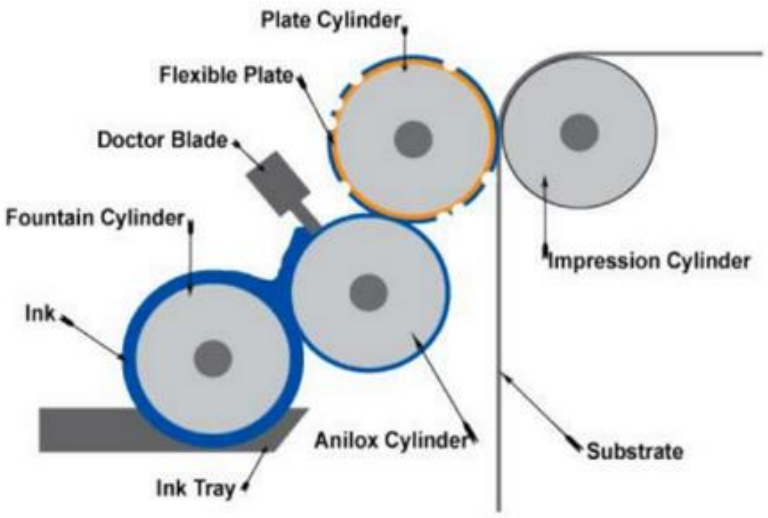

Figure 3.1 Scheme of flexographic printing technique. Adapted from [41].

The *Kromekote*® S1 paper is a one-face coated, calendared paper using a hot chrome-plated cylinder to bring brightness and a smooth surface to ensure a better printing resolution. The paper substrate is pre-patterned with a printed silver-based ink electrode. Three types of patterns are used, with an electrode distance of 100, 150 and 200 µm, which are also printed by flexography. The influence of shellac cross-linking on electrical response was studied with and without thermal treatment: the Sepia-shellac samples are measured before and after thermal treatment (3 days after printing). The thermal treatment involved samples placed onto a hot plate for 1 hour at 70 °C.

For fundamental studies, ink deposition was made by spin coating in ambient conditions of 30 to 70 µl at 3000 rpm for 1 min onto gold patterned SiO_2 substrates. The substrates are pre-washed before spin coating following a cleaning protocol with sonication bath steps through solvents (deionized water, acetone, and isopropanol) and UV-ozone surface cleaning to remove last impurities and dust (*Appendix A*). The spin-coated films were let drying for 1 h in both ambient conditions and inert conditions (N_2 atmosphere glove box < 3 ppm H_2O and O_2).

3.2 Substrate, printed film, and electrical characterization

3.2.1 Grammage

The grammage is a key measurement for paper and printed samples characterization.

From office paper to cardboard, grammage is not only a measurement, but also a tool to normalize other measures especially for mechanical tests such as traction, shear and burst resistance. It is also used to normalize or calculate indexes for physicochemical measures, such as air permeability, roughness, and porosity. The papermaking industry and researchers introduced grammage as a common language regarding the characterization and normalization of paper properties. It can give information about paper pulp during the papermaking process, especially the amount of water in the pulp sheet and the dryness of the final paper sheet. Knowing and controlling the grammage of paper is essential to adapt the production parameters depending on the type of paper produced and its purpose. Indeed, the grammage is somehow proportional to the thickness of the sheet, and so influences the mechanical properties [42]. It is defined as a surface mass, usually referred as G (g/m²), it can be determined from the weight m (g) for a specific area S (m²), but also from the density ρ (kg/m^3) and thickness *thickness* (m) [42], [43]:

$$G = \frac{m}{S} = \frac{m}{V} \times thickness = \rho \times thickness \tag{3.2.1}$$

In general, the grammage is measured over 10 samples for an area of 10 cm² using a pattern to cut samples. In the case of this study, the printed film does not exceed 10 cm², and so, a made-to-measure pattern in glass is used to fit the shape of the sample. For the bare paper substrate, it was a 73 cm² pattern and 9.3 cm² for the printed sample. The weight is measured three times for each sample, and the values is taken 5 s after sample deposition on the balance's plate (stabilization time) with the analytical balance *Mettler Toledo XPR204*, following the ISO 536:2012 standard: Paper and board — Determination of grammage [43]. Grammage is measured in this study for 10 bare paper substrates samples, 6 for non-cross-linked (without sintering treatment) Sepia-shellac printed on paper, and 6 for cross-linked (with sintering treatment) Sepia-shellac printed on paper.

3.2.2 Thickness of the films

Thickness is an essential element of knowledge to estimate conductivity by electrical measurements.

Two different methods are used depending on the substrates. For samples on SiO_2, measurements were made with a profilometer DEKTAK. For paper substrates, the measurements were made with a micrometer *49-86-TMI* (*Testing Machine*) according to the standard TAPPI T-411 (hammer speed of 1 mm/s and pression of 50 kPa) with a precision of 1 µm [44]. Three measurements at different positions were taken on each sample, for the printed samples with the *49-86-TMI-micrometer* (10 samples of bare paper, 6 samples of non-cross-linked printed Sepia-shellac and 6 samples of cross-linked printed Sepia-shellac).

3.2.3 Water absorption: Cobb index

The effect of thermal treatment on printed Sepia-shellac samples are made complementary through electrical and physicochemical measurements. The properties of shellac (amphiphilicity) make relevant the use of water absorption and wettability characterization of the printed films.

The water absorption of paper substrates and printed samples with a recommended grammage higher than 50 g/m² can be estimated with the Cobb test. This test provides the amount of water absorbed for a specific time and surface.

When the $Cobb_{60}$ test is used, it implies that water absorption is measured for 60 seconds. The sample is weighed before exposure to water and placed on a metallic plate where a ring is set to contain water and avoid leakage (Figure 3.2). The ring area is 10 cm², and the amount of water poured in it is 10 ml. Once the water is poured, the chronometer is gone off for 60 sec, and then the plate is turned over to remove the water.

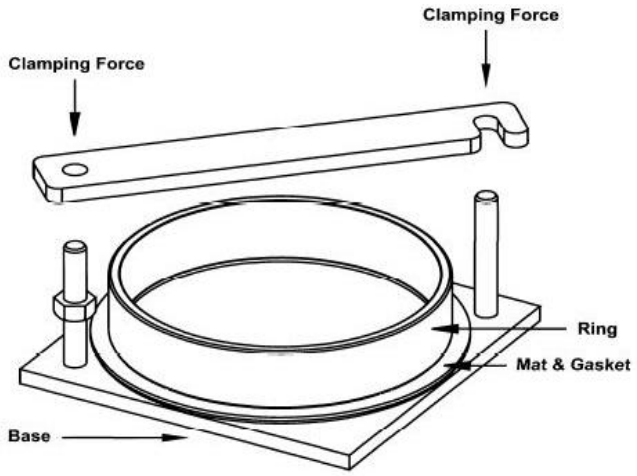

Figure 3.2 Scheme of Cobb test for water absorption determination. Adapted from [45].

The sample is recovered, and placed under a blotting paper, the passage of a roller allows to absorb the excess of water on the surface of the sample. The sample is then weighed at the end of the process, and the Cobb index (g/m²) can be calculated with the initial weight of the sample m_1 (g), the final weight m_2 (g) and the ring area S_r (m²) [45]:

$$Cobb_{60}Index = \frac{m_2 - m_1}{S_r} \tag{3.2.3}$$

Usually, the printed samples are compared with the bare paper substrate as reference. This test is made following the ISO 535:2023(en) standard: Paper and board — Determination of water absorptiveness — Cobb method [45]. The weight is measured three times for each sample, and the values are taken 5 s after sample deposition on the balance's plate (stabilization time) with the analytical balance *Mettler Toledo XPR204*. The Cobb index was measured in this study for 10 bare paper substrate samples, 6 non-cross-linked (without sintering treatment) Sepia-shellac printed on paper, and 6 cross-linked (with sintering treatment) Sepia-shellac printed on paper.

3.2.4 Contact angle

The contact angle measurement permits to characterize the affinity of a liquid for a solid surface translating a thermodynamic equilibrium between three phases and interfaces: substrate-liquid (solid-liquid), substrate-atmosphere (solid-gas), and liquid-atmosphere (liquid-gas). This test can be used to study the wettability, hydrophobicity and hydrophilicity of a liquid or solution for a specific surface. Indeed, the contact angle at equilibrium θ_0 (rad) can give access to interfacial tensions (J/m² or N/m) between liquid and solid γ_{SL}, solid and gas γ_{SG}, and liquid and gas γ_{LG}, with the Young's equation [46], illustrated on Figure 3.3:

$$\gamma_{SG} = \gamma_{SL} + \gamma_{LG} cos\theta_0 \tag{3.2.4}$$

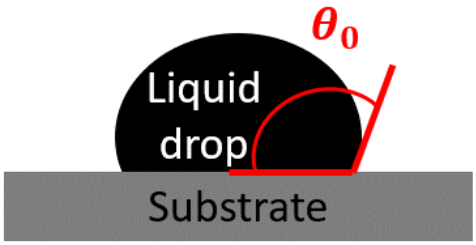

Figure 3.3 Scheme of the contact angle measurements at equilibrium.

The contact angle was measured with the optical tensiometer *Dataphysics OCA-20*. The sample is placed on the plate and fixed with two weights on the edges to ensure the paper sheet is horizontal. A drop of liquid is released on the sample and acquired with a camera for 10 seconds. The picture analyzed is the one taken at the end of the 10 seconds, the time for the drop to stabilize. The *Dataphysics* software enables recognition of the drop's contour and the baseline between the drop and the substrate. This allows then to estimate the drop's radius, volume, and contact angle, which is the angle formed between the drop-substrate baseline and the tangent at the contact point between drop and the substrate. This measurement was initially realized with 5 µl-water drops for six substrates: bare paper and SiO_2 substrates (as a reference), printed non-cross-linked Sepia-shellac and printed cross-linked Sepia-shellac on paper and SiO_2 to study the effect of the thermal treatment on wettability. Afterwards, the contact angle was measured with Sepia-shellac and commercial Sepia inks, with a 5 µl-drop on bare paper and SiO_2 substrates. Each of these measurements were made twice, for reproducibility.

3.2.5 Scanning Electron Microscopy

Scanning Electron Microscopy (SEM) was used for nanoscale characterization, with a maximum resolution of about 0.3 nm (for optical microscope it is about 200 nm). The depth of observation depends on the energy of the electron beam. Usual source for electron beam generation is tungsten, the beam is focused through several magnetic lenses. Images are usually taken for an incident electron beam voltage between 1 and 30 kV [47].

SEM features chemical contrast observations by the analysis of backscatter electrons (high energy) generated by elastic scattering interactions (deviation) with the sample's matter. In addition, topographic contrast is observed through detection angle of secondary electrons (low energy) resulting from inelastic scattering interactions (expulsion of another electron when entering atom electronic shell) with the matter (Figure 3.4).

For insulating materials, the Environmental Scanning Electron Microscopy (ESEM) provides observations without requirements of coating samples with an aluminum or gold film. The surface is *neutralized* by local injection of gas (air) that generate positive ions, preventing electron accumulation [48]. This mode suits for paper substrates characterization.

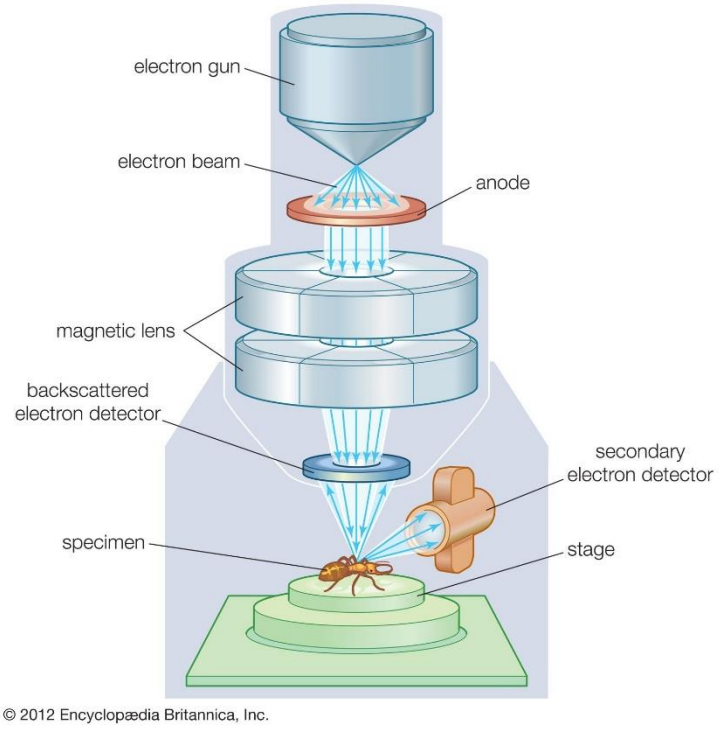

Figure 3.4 Scheme of Scanning Electron Microscopy (SEM). Adapted from [49].

3.2.6 Electrical characterization

For the electrical characterization, two main methods are used in this study: current-voltage (I-V) and current-time potentiostatic (I-t) characteristics for Sepia-shellac, commercial and natural ink.

For printed Sepia-shellac, I-V characteristics were obtained from two types of electrode patterns, with different interelectrode distances (100, 150 and 200 µm). Overall, 6 samples were studied. Details on the electrodes are described in Chapter 4. The measurements were carried out from 0 V to 10 V, at 100 mV/s. The influence of thermal treatment was studied with 2 Sepia-shellac printed samples on paper with an interelectrode distance of 100 µm. Current-voltage I-V measurements, from 0 V to 10 V at 250 mV/s with 3 cycles, were made on these two samples before and after thermal treatment (at 70 °C for 1 hour).

With commercial ink, samples spin coated on SiO_2 using the protocol for ink deposition (Chapter 3, section 1), we prepared 5 samples in a dry N_2 glove box, where samples were also measured. It was made by I-V from 0 V to 2 V at 5, 25, 50, 100 and 250 mV/s, with three I-V cycles. These measurements were repeated in ambient, humid (80 % relative humidity), and ambient conditions again, with 24 h-delay (in the following atmosphere) between each type of atmosphere.

To compare the behavior of commercial and natural ink, I-V characteristics were measured from 0 V to 0.5 V, for 3 cycles, at 1, 10 and 100 mV/s. I-t (potentiostatic) characteristics were also measured for 900 sec at 0.1 V, 0.5 V, 1 V and 2 V. Deionized water was added to the natural ink to facilitate the spin coating process: 0.37 g of natural ink were mixed with 0.12 g of deionized water, under stirring at 400 rpm for 30 min. The resulting mixture was spin coated at 1000 rpm, for 1 min and let drying for 30 min.

All the electrical measurements were acquired using an *Agilent – Keysight B1500A Semiconductor Parameter Analyzer* and a home made micromanipulated electrical probe station. The conductivity σ ($S.cm^{-1}$) can be estimated with the interelectrode distance L (cm), the cross-section area A (cm^2) and the film electrical resistance R (Ohm). The cross-section area is calculated with the electrode length l and film thickness (with electrode height, 50 nm) W. The electrical resistance can be found by the current I (A) at potential V (V) in the hypothesis of ohmic conditions [8], the terms are illustrated on Figure 3.5.

$$\sigma = \frac{L}{A \times R} = \frac{L}{(l \times W) \times \frac{V}{I}} \tag{3.2.6}$$

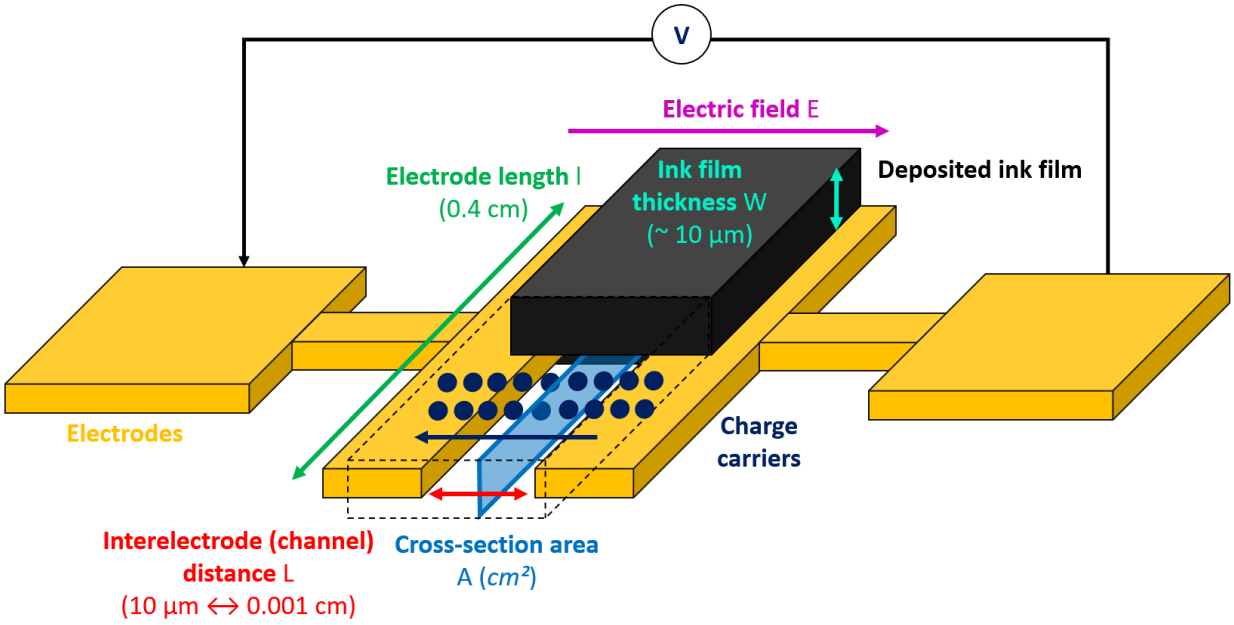

Figure 3.5 Scheme of the electrode pattern, film deposition on the electrodes and electrical measurement setup with related terms to estimate conductivity.

CHAPTER 4 RESULTS AND DISCUSSION

4.1 Sepia-shellac ink and printed films characterization

In the first place we present the results of the characterization of Sepia-shellac ink, substrates, and printed films. Results obtained by NAA about elemental composition of extracted Sepia melanin powder and Sepia-shellac ink formulated from this powder are presented in the first section. Later, we discuss substrate and thin film properties as studied by SEM, grammage, thickness, Cobb index and contact angle. The last part focuses on electrical response of printed Sepia-shellac ink on paper, including the influence of thermal treatment.

4.1.1 Extracted Sepia melanin powder and Sepia-shellac ink elemental composition

NAA results are key to determine the extraction efficiency of Sepia melanin powder and potential contamination of Sepia-shellac ink.

The NAA results are given in ppm, which corresponds to the µg of the detected element over the entire weight of the sample, in g. The results in Table 4.1 show the presence of sulfur, silicon, sodium, chlorine, iron, aluminum, potassium, calcium, and magnesium (from the most to the less concentrated). Indeed, Sepia melanin has binding affinity for metal ions, which can lead to binding through chelation and Coulomb interactions [28]. Such interactions explain the presence of these elements even after extraction and purification of Sepia melanin. The highest concentrations are for silicon, sodium, chlorine, and sulfur, possibly explained by the environment in which cuttlefishes live. Before releasing ink jet to blind predators, the first behavior cuttlefishes use to stay safe is digging in sea sand. This sand contains sediments (sulfuric, silicon) and salts (sodium, chlore) also present in sea water [50], which can explain the presence of these components in higher concentrations than for other elements. Some of these components are also naturally present in the melanogenesis of cuttlefish ink as some proteins contain sulfur. Indeed, natural Sepia melanin ink from cuttlefish is known to contain 15 w% of eumelanin and 5 to 8 w% of proteins [51].

Table 4.1 Elemental composition of extracted Sepia melanin powder and Sepia-shellac ink obtained by Neutron Activation Analysis.

Element	***Extracted Sepia melanin powder***		***Sepia-shellac Ink***		***Detection limit (ppm)***
	Value (ppm)	*Uncertainty (ppm)*	*Value (ppm)*	*Uncertainty (ppm)*	
Na	**2093**	**110**	**169**	**11**	<0.002
Mg	**93,1**	**27,6**	**24,9**	**6,9**	<1
Al	**229**	**11**	**33,5**	**1,7**	<0.01
Si	**<2600**	**-**	**<410**	**-**	<30
S	**2688**	**968**	**399**	**166**	<2
Cl	**843**	**40**	**207**	**9**	<0.05
K	**130**	**27**	**115**	**9**	<0.05
Ca	**117**	**20**	**30,4**	**3,5**	<0.3
Sc	<0.1	-	<0.02	-	<0.002
Ti	13,6	2,8	3,25	0,51	<0.1
V	0,305	0,021	0,0577	0,0044	<0.001
Cr	8,07	1,91	2,85	0,39	<0.1
Mn	15,4	0,7	3,81	0,16	<0.002
Fe	**<580**	**-**	**<130**	**-**	<5
Co	14,3	0,9	1,20	0,11	<0.05
Ni	<80	-	<20	-	<2
Cu	14,6	1,3	3,79	0,28	<0.05
Zn	<40	-	<6	-	<0.05
As	1,32	0,08	0,147	0,011	<0.0005
Se	<5	-	<2	-	<0.01
Br	37,8	1,5	4,06	0,17	<0.0005
Rb	<20	-	<3	-	<0.2
Zr	**<430**	**-**	**<50**	**-**	<0.1
Mo	<2	-	<0.3	-	<0.02
Ag	***<0.8***	**-**	***2,53***	***0,18***	<0.02
Cd	<2	-	0,195	0,056	<0.02
In	<0.008	-	<0.0009	-	<0.0001
Sn	***<5***	**-**	***5,68***	***0,45***	<0.1
Sb	<0.05	-	<0.008	-	<0.0005
I	0,985	0,098	0,155	0,014	<0.002
Cs	<0.8	-	<0.3	-	<0.02
Ba	<60	-	<9	-	<0.1
La	<0.2	-	0,0201	0,0043	<0.002
Hf	<0.5	-	0,179	0,037	<0.01
W	<0.2	-	0,112	0,015	<0.0005
Au	<0.003	-	<0.0009	-	<0.0001
Hg	<0.4	-	<0.08	-	<0.005
Th	<0.3	-	<0.05	-	<0.005
U	<0.2	-	<0.05	-	<0.001

The concentrations of the above-mentioned elements are reduced by 1.13 to 12.38 for Sepia-shellac ink, except for silver and tin. This can be explained by the addition of shellac and 1-propanol, mainly composed of carbon, hydrogen, and oxygen, which leads to a decrease of the concentrations observed as extracted Sepia melanin powder concentration in the formulated ink is 22.62 w%.

Concerning the higher amount of silver and tin in the Sepia-shellac ink, this can be due to contamination during the ink formulation process or storage. Some values do not feature uncertainty because of low signal, neighboring the detection limit, or due to noise that does not allow to have proper fit of the model to estimate the amount of the element present.

In this case, the largest fit is chosen, that is why the value given is expressed as inferior as the highest value of the fit. Noise and backscatter noise can be generated by some elements such as sodium and so hide entirely or in part other signals coming after, of lower energy (keV) during the counting step [39], [40], [52]. Indeed, high uncertainties are observed for magnesium and sulfur. The presence of sodium chloride especially affects the discernability of the magnesium peak. For sulfur, it is mainly due to a weak detection efficiency because of the narrow spectral gamma ray intensity (at 3102 keV), which induces weaker peaks' area and so higher uncertainty.

4.1.2 Ink rheology and wettability

After the characterization of the chemical composition of the Sepia melanin-based ink, the formulated Sepia-shellac ink printability is characterized by the measurement of viscosity and ink contact angle, both on paper and SiO_2 substrates.

The usual range for dynamic viscosity in flexographic printing is between 0.01 and 0.1 Pa.s [23]. Here at 1200 s^{-1}, the dynamic viscosity is about 0.25 Pa.s and yet induces no printing defects as regular flexographic press was not used, but lab-scale flexographic printer which allows wider viscosity range.

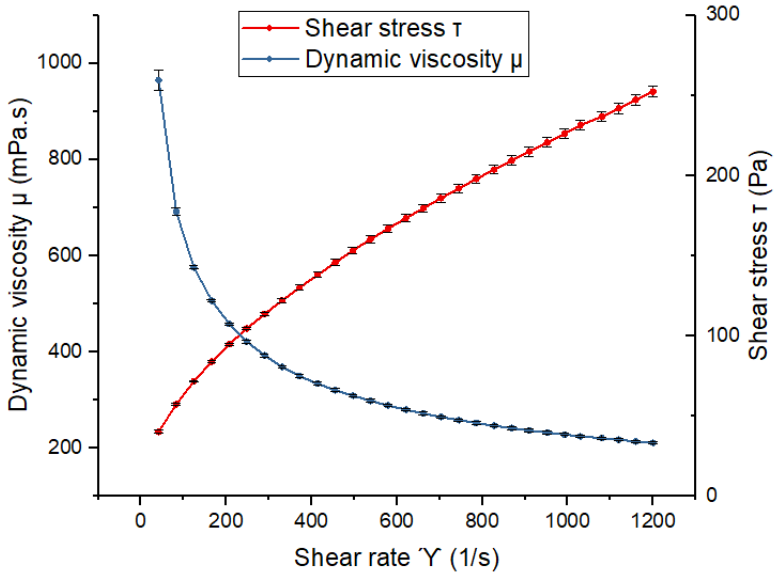

Figure 4.1 Dynamic viscosity and shear stress of Sepia-shellac formulated ink obtained by rheologic test.

Besides, this rheologic test, through the shape of the curves shown on Figure 4.1, indicates a clear shear thinning fluid behavior for the Sepia-shellac ink. It means that with an increasing shear, the viscosity diminishes, in other words, the energy required to put in movement the same amount of fluid (flow resistance) decreases through time. This type of behavior is common for inks and paints. It can be explained in the case of the Sepia-shellac ink by the presence of Sepia melanin in shellac and 1-propanol matrix. Indeed, when the fluid is at rest particles can be bound by weak interactions such as Van der Waals or hydrogen bonding, which are gradually broken when shear is applied [53], [54].

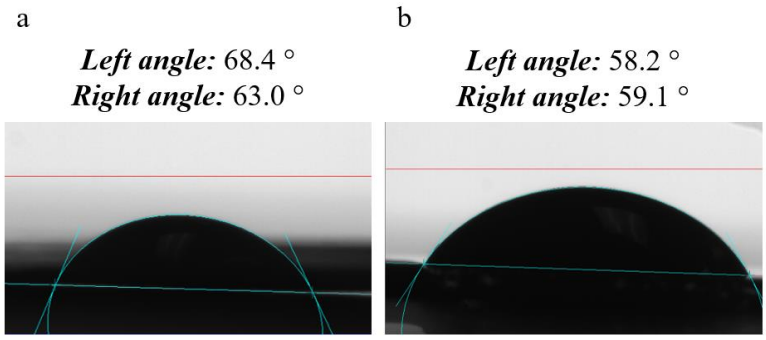

Figure 4.2 Contact angle captures of Sepia-shellac ink on paper substrate (a) and SiO_2 substrate (b).

The contact angle (Figure 4.2) is lower and indicates better wettability for Sepia-shellac ink dropped on SiO_2 substrates compared to paper ones (i.e., lower interfacial tension between the ink drop and the solid substrate). This might be due to the UV-ozone treatment that can enhance wettability and remove surface dust and impurities, while for paper such treatment is not possible as it can induce paper ageing [55], [56]. Dust and impurities can form a thin layer at the surface of the sample and so modify the surface properties [56]. Further, these contact angle measurements were made only once per type of sample, as preliminary results. Additional measurements are required to improve the reliability of the results.

4.1.3 Substrate and printed film characterization

After the Sepia-shellac ink characterization, to ensure it has the proper viscosity for printing, we proceeded to a SEM study to image the Sepia-shellac printed film on paper focusing the attention on the possible presence of surface defects. The study of the printed film characteristics is key to shed light on films' electrical responses. The printed Sepia-shellac film on paper features cracks clearly visible on Figure 4.3 (b) but not visible with bare eyes Figure 4.3 (a). These cracks of about 1-2 µm width can affect the electrical response as it generate an important separation of Sepia melanin granules compared to their size about 100 to 200 nm. Electrical response is still observed, so there was no way to characterize cracks impact as they are formed by the Sepia-shellac ink drying just after printing due to the difference of mechanical properties between the substrate (paper) and the printed film.

Moreover, cracks can also be generated by the drying shrinkage due to contraction of fibers from the paper during the drying process. Indeed, paper is humidified by the ink application during printing which induces a relaxation of the fibers. Fibers become more conformable as they can form a higher number of H-bondings with the solvent of the ink. When the solvent evaporates and the paper dries, the fibers take back their original forms by shrinkage [57]. However, the printed film is not subjected to shrinkage, or way lesser, which leads to a curvature of the paper and the film due to the shrinkage force of the paper. This curvature provokes cracks. The electrical response can be impacted resulting by a possible lower conductivity. The picture (b) shows how shellac contributes to Sepia granules dispersion homogeneity by the embedding of the granules in the shellac matrix.

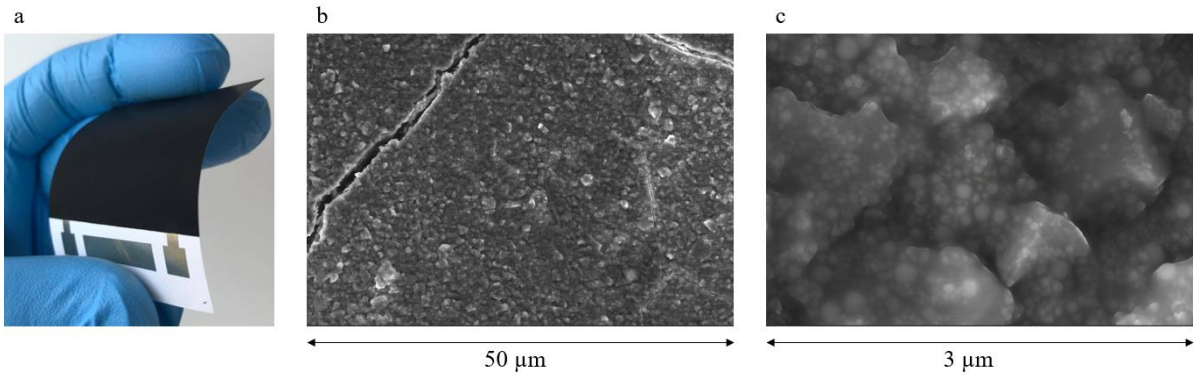

Figure 4.3 Printed Sepia-shellac film on paper pictures (a) entire sample, (b) by SEM 50 µm and (c) by SEM 3 µm.

Grammage and thickness gives information about dimensions and weight of the printed film, Figure 4.4. The grammage average is 74.90 g/m² for bare substrate paper, 82.57 g/m² for cross-linked (thermal treatment at 70 °C for 1 h), and 80.10 g/m² for non-cross-linked Sepia-shellac. The grammage average shows the cross-linked and non-cross-linked Sepia-shellac films represent around 9.3 w% and 6.5 w% respectively of the printed sample. No significant impact is observed concerning grammage due to shellac cross-linking (after the thermal treatment as mentioned in Chapter 2 and 3) according to the average values and the standard deviation.

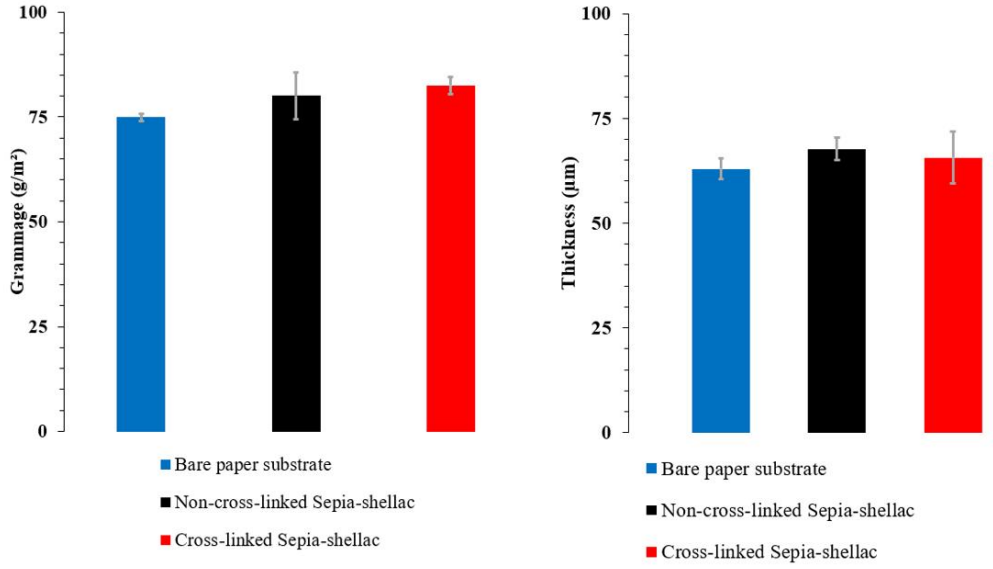

Figure 4.4 Grammage and thickness of paper substrate and printed film of cross-linked and non-cross-linked Sepia-shellac on paper.

The average thickness on Figure 4.4 of the printed film is about 4.7 µm for non-cross-linked Sepia-shellac and 2.6 for cross-linked Sepia shellac. The average thicknesses of these films were obtained by subtraction of the average paper thickness to the average paper and printed film thickness. The average thickness was estimated through measurements in the three different points for each of the 10 samples of bare paper, 6 samples of non-cross-linked printed Sepia-shellac and 6 samples of cross-linked printed Sepia-shellac. These values are lower than the usual ones obtained by flexographic printing for film thickness presented in Chapter 3, as explained in the previous section, this is due to the printer used, which is lab-scale and not regular press. This might also induce heterogeneity in printing as the lab-scale printer tank needs to be refill and so even with the blade, just after refilling, more ink might be present on the applicator roll. The sample printed just after printer tank refilling might have higher thickness than the ones printed after with less ink on the applicator roll. However, the standard deviation indicates that the values for cross-linked Sepia-shellac might not be that different compared to non-cross-linked. In this sense, it is not possible to confirm the cross-linking of shellac induces a film thickness diminution.

4.1.4 Influence of a thermal treatment on water absorption and surface hydrophobicity

The impact of a thermal treatment is characterized by electrical measurements in next Chapter and by contact angle and Cobb test to give additional information to consider the thermal treatment effect hypothesis. Indeed, shellac, when brought to 70 °C, tends to soften and allows the sintering and migration of Sepia melanin granules near the electrode interface. Therefore, shellac becomes mainly located at the surface of the printed film. As presented in Chapter 2, shellac contains major hydrophobic segments. While Sepia melanin, despite being poorly soluble, features hygroscopic properties. In this sense the thermal treatment should affect both the printed film surface and interface with electrode. Concerning the surface, as shellac is in majority present, the water absorption should decrease. Observations of Cobb test results, shown on Figure 4.5, highlight the diminution of the amount of water absorbed by the sample for cross-linked compared to non-cross-linked Sepia-shellac, with paper as reference. The standard deviation still indicates an important dispersion of the measured values, especially for non-cross-linked Sepia-shellac. It is also important to note that few deviations in films' thicknesses can induce non-negligible changes in

the film. This result suggests that the deviations of the films' thicknesses observed on Figure 4.4 might be important enough to induce water absorption capacity of the paper and the printed films.

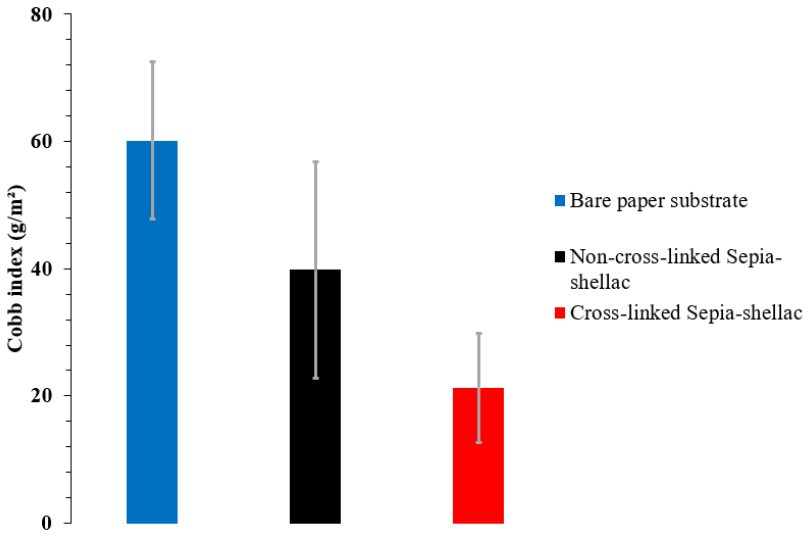

Figure 4.5 Cobb index of paper substrate and printed film of cross-linked and non-cross-linked Sepia-shellac on paper.

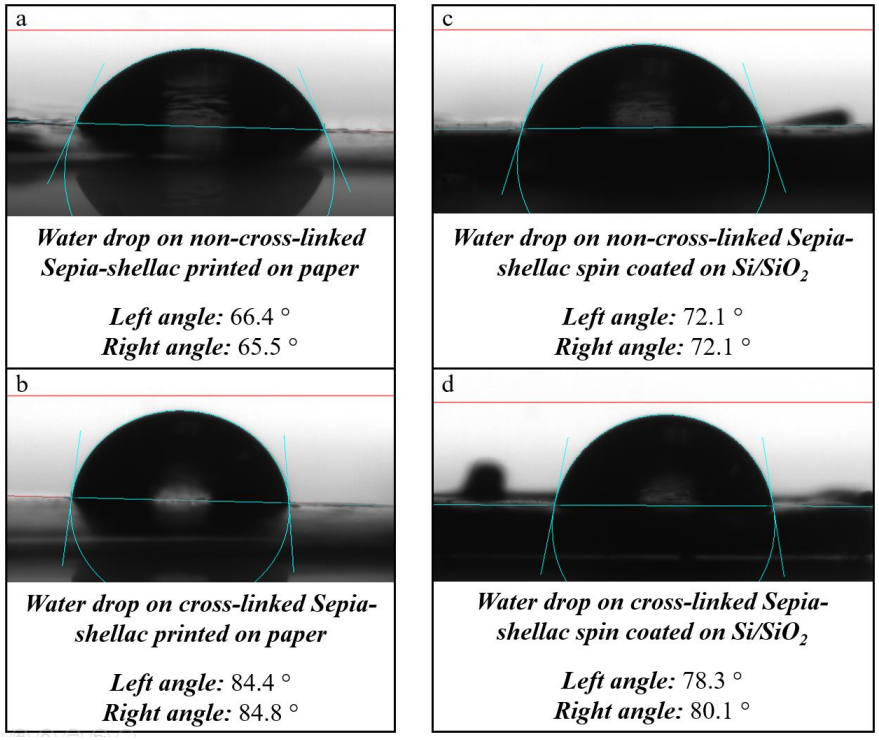

Figure 4.6 Contact angle pictures of water drop on (a) non-cross-linked and (b) cross-linked Sepia-shellac printed film on paper, (c) non-cross-linked and (d) cross-linked Sepia-shellac spin coated film on SiO_2.

For both Sepia-shellac ink printed on paper and spin coated on SiO_2 substrates, the contact angle increases for those cross-linked by heating at 70 °C for 1 hour, presented on Figure 4.6, supporting the attribution described for Cobb test results.

It appears as cross-linking on paper contributes to more Sepia granules agglomerated at the electrode interface and shellac presence near the surface, with a higher contact angle compared to SiO_2 substrates. However, to confirm this hypothesis more values are required to establish a proper average and take standard deviation into consideration. Indeed, this change is contact angle can also be due to paper deformation through the heating process at 70 °C inducing some water evaporation and so shrinkage as discussed in the previous part [57]. Also considering the difficulty to keep a flat surface for paper during contact angle measurement, that is why a not or weakly deformable substrate (in ambient conditions) as SiO_2 is taken as reference. Further, these measurements were held only once for each type of samples: more measurements are required for better reliability.

4.2 Electrical characterization of Sepia-shellac printed films on paper

The first electrical measurements were made on printed Sepia-shellac samples with three different electrodes patterns with interelectrode distance of 100, 150 and 200 µm (Figure 4.7). The highest values of the current were reached with samples with an interelectrode distance of 100 µm. Lower current is obtained for wider electrode distance, except for samples 3 (S3 – 150 µm) and 4 (S4 – 150 µm) compared to sample 6 (S6 – 200 µm), possibly due to printing defects [16].

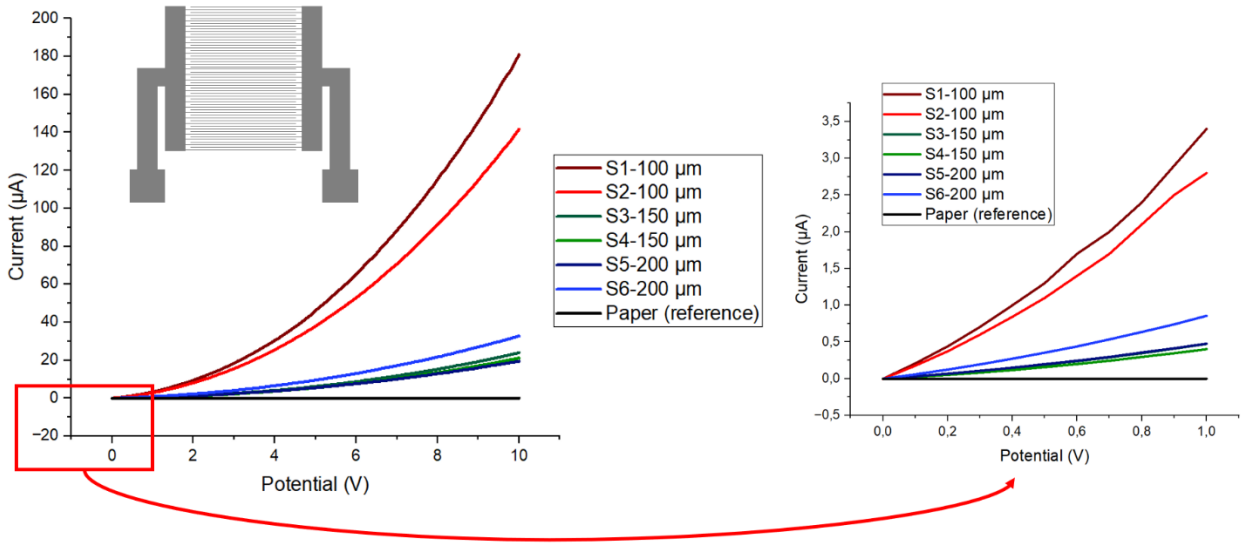

Figure 4.7 Current-voltage (I-V) measurements of Sepia-shellac films printed on paper with different interelectrode distances (100, 150 and 200 µm) from 0 V to 10 V, at 100 mV/s in ambient conditions (left), optical images of the electrode patterns (right).

The shape of the curves shows a non-linear increase of the current. In other words, in the range of potential investigated, the samples do not show a typical resistor behavior. The non-ohmic behavior is attributable to interface instability caused by charge carrier traps (space-charge layer at the interface [58]). The order of magnitude of the current observed at 10 V for the Sepia-shellac films printed on paper is the same as the one presented in reference [8], where, for an interelectrode distance of 100 µm and 150 µm, the current reached around 800 µA and 200 µA, respectively, for Sepia-PVB printed film on paper. The results indicate strong similarities, showing that similar results can be obtained with a bio-sourced binder as shellac instead of PVB. The dimensions used to calculate the cross-section area are 25 cm for the electrode pattern (shown on Figure 4.7) for the electrode length l and 4.7 µm (estimated in Figure 4.5) for the film thickness W. For the results on Figure 4.7, the conductivity at 0.5 V for interelectrode distances of 100 µm, 150 µm and 200 µm taken for the average current is respectively about $2.0 \times 10^{-6}\ S.cm^{-1}$, $4.4 \times 10^{-7}\ S.cm^{-1}$ and $9.4 \times 10^{-7}\ S.cm^{-1}$.

4.3 Influence of thermal treatment on electrical response

Figure 4.8 illustrates the electrical response of two samples of Sepia-shellac printed films on paper substrates, before and after thermal treatment. The thermal treatment was processed at 70 °C for 1 hour, three days after printing. An increase of the electrical conductivity around one orders of magnitude is observed at 10 V after thermal treatment. Indeed, for the samples with a non-cross-linked Sepia-shellac (NCL) film, the current at 10 V is comprised between 10 µA and 100 µA ($4.0 \times 10^{-6}\ S.cm^{-1}$ conductivity), while for the cross-linked (CL) ones it reaches 800 µA to 1.1 mA ($1.4 \times 10^{-4}\ S.cm^{-1}$ conductivity). The thermal treatment of the films softens the shellac matrix and might facilitate the aggregation of the Sepia melanin granules. In turn, this might lead to a sort of densification of the Sepia melanin, paralleled by an increase in the number of the possible percolation paths. To compare the conductivity with results obtained in Figure 4.7, the conductivity at 0.5 V for non-cross-linked and cross-linked samples are respectively about $6.3 \times 10^{-7}\ S.cm^{-1}$ and $4.2 \times 10^{-5}\ S.cm^{-1}$.

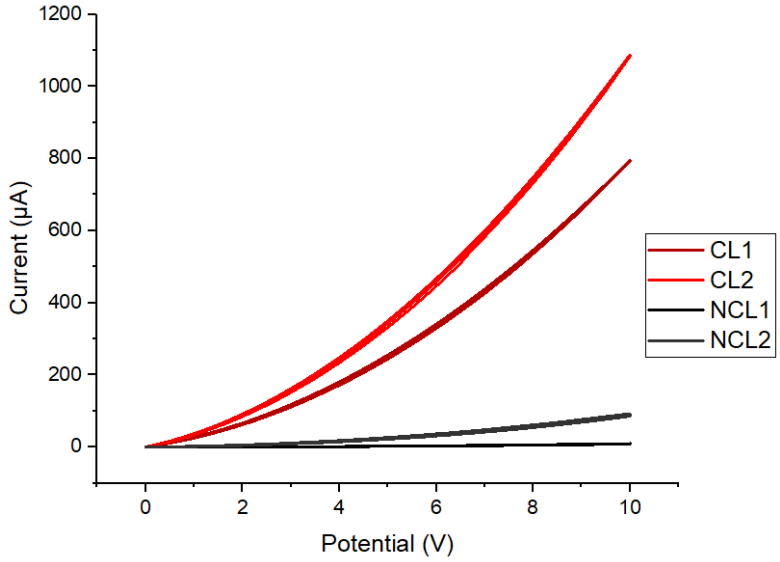

Figure 4.8 Electrical characterization by current-voltage (I-V) measurements of non-cross-linked (NCL) and cross-linked Sepia-shellac (CL) films printed on paper from 0 V to 10 V, at 250 mV/s for 3 cycles, in ambient conditions.

These results suggest a potential application of Sepia-shellac samples as temperature sensors. Indeed, the thermal properties of shellac, allowing softening in the film, open the possibility for the temperature to control the electrical response.

4.4 Natural and commercial Sepia melanin inks characterization

4.4.1 Elemental composition

The presence of certain chemical elements in Sepia melanin depends on several factors, such as sampling protocol and ink synthesis conditions in the cuttlefish, in turn affected by age of the cuttlefish, geographic fishing zone, fishing season of the year, temperature and pH during synthesis, genetic background, etc.

The NAA results reported in Table 4.2 for natural (raw) and commercial (with NaCl added by food-processing manufacturer) Sepia melanin ink, compared to the extracted Sepia melanin and Sepia-shellac ink, indicate that the same elements are present at the highest concentrations.

The results for the commercial ink show higher uncertainty values due to the high concentration of sodium chloride which causes noise in the spectra. The high amount of sodium chloride in the commercial ink, is probably due to the salt added in it during the manufacturing process as it is destined for agri-food industry. The noise affects the detection of peaks such that only a rough estimation can be made for the concentrations of silicon, iron, sulfur, nickel, zirconium, rubidium, zinc, and potassium.

Concerning the natural Sepia melanin ink, the main elements we found, except for sodium chloride, are magnesium, silicon, sulfur, potassium and calcium.

Some metals are also found in the natural ink, but in lower amounts than in the commercial ink such as aluminum, titanium, iron, copper, arsenic, zirconium, and tin, except for bromine which has higher concentration in natural one. These differences might be due to natural ink synthesis conditions, mentioned above (first paragraph, section 4.1.1). The commercial ink being produced in food-processing industrial conditions, cross contamination can occur, leading to higher amounts for these elements. This contamination can also be originated from the sodium chloride salt added during the manufacturing of the commercial ink.

Table 4.2 Elemental composition of natural and commercial Sepia melanin inks.

Element	***Natural Sepia melanin Ink***		***Commercial Sepia melanin Ink***		***Detection limit (ppm)***
	Value (ppm)	*Uncertainty (ppm)*	*Value (ppm)*	*Uncertainty (ppm)*	
Na	**8196**	**328**	**69361**	**2783**	<0.002
Mg	**9041**	**387**	**2088**	**263**	<1
Al	<60	-	<280	-	<0.01
Si	**<8700**	-	**<42000**	-	<30
S	**<7400**	-	**<32000**	-	<2
Cl	**8111**	**382**	**100205**	**4016**	<0.05
K	**2213**	**147**	**<5100**	-	<0.05
Ca	**6714**	**307**	**1927**	**253**	<0.3
Sc	<0.003	-	<20	-	<0.002
Ti	<20	-	<100	-	<0.1
V	<0.2	-	<0.7	-	<0.001
Cr	<0.3	-	<900	-	<0.1
Mn	0.538	0.076	2,23	0,38	<0.002
Fe	<50	-	**<160000**	-	<5
Co	<0.8	-	<390	-	<0.05
Ni	<5	-	**<17000**	-	<2
Cu	18.0	4.1	<50	-	<0.05
Zn	3.82	0.45	**<5000**	-	<0.05
As	12.2	0.5	<10	-	<0.0005
Se	<0.3	-	**<1000**	-	<0.01
Br	58.7	2.4	18,6	2,3	<0.0005
Rb	<2	-	**<3000**	-	<0.2
Zr	<20	-	**<64000**	-	<0.1
Mo	<0.3	-	<180	-	<0.02
Ag	<5	-	<20	-	<0.02
Cd	<0.5	-	<230	-	<0.02
In	<0.03	-	<0.1	-	<0.0001
Sn	<20	-	<100	-	<0.1
Sb	<0.009	-	<5	-	<0.0005
I	<2	-	<3	-	<0.002
Cs	<0.09	-	<230	-	<0.02
Ba	<6	-	<120	-	<0.1
La	<0.03	-	<8	-	<0.002
Hf	<0.03	-	<100	-	<0.01
W	<0.2	-	<30	-	<0.0005
Au	<0.0007	-	<0.5	-	<0.0001
Hg	<0.3	-	<90	-	<0.005
Th	<0.02	-	<60	-	<0.005
U	<0.06	-	<2	-	<0.001

4.4.2 Ink rheology and wettability

Regarding inks' rheology and wettability, the viscosity and contact angle measurements were only performed on commercial Sepia melanin ink (Figure 4.10). This is due to the limited availability of natural Sepia melanin ink, whose use was mainly for electrical measurements.

The commercial ink shows a similar behavior for viscosity compared to the Sepia-shellac one, the same shear thinning fluid behavior is observed. Besides, the viscosity is about 0.2 Pa.s at 1200 s^{-1}, the same order of magnitude as Sepia-shellac ink. The properties of the commercial ink are such that it could be possible to use it with the lab-scale flexographic printer and so will, thus avoiding ink formulation steps. In this sense, economy of energy and chemicals can be foreseen.

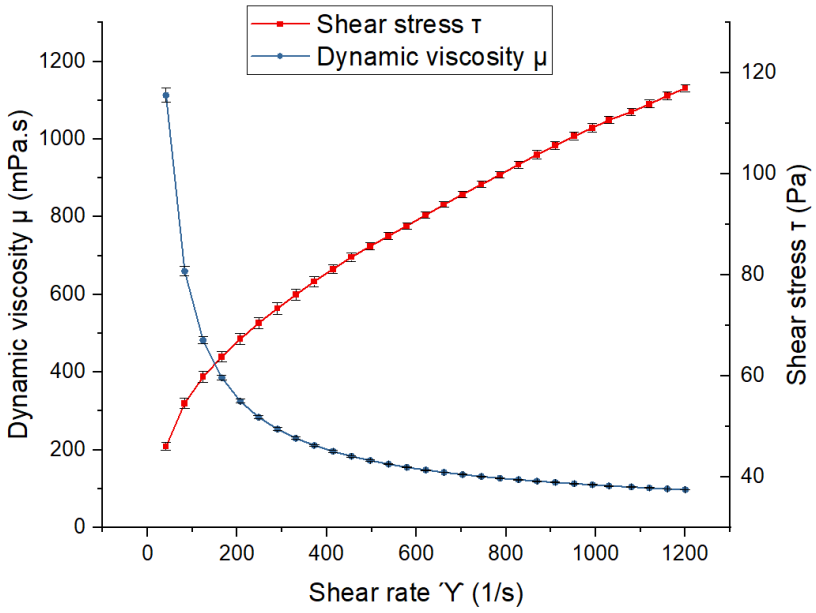

Figure 4.9 Dynamic viscosity and shear stress of commercial ink vs shear rate, obtained by rheological tests.

The observations deduced from the rheology tests are in agreement by those obtained from contact angle tests (Figure 4.11). The wettability is similar for both inks. On SiO_2 substrates, the contact angles (left and right) are similar to those for Sepia-shellac ink: 58.8° and 65.3° (commercial ink) compared to 58.2° and 59.1° (Sepia-shellac).

On paper substrates, the difference in the measured angles is larger: the angles are 79.3° and 79.7° for commercial ink and 68.4° and 63.0° for Sepia-shellac. The angle variation is probably caused by the difficulty to keep the substrate flat during the measurement that would generate blurred images (the image would then be more difficult to analyze thus causing errors due to baseline settings). The flatness of the substrate is also influencing the difference of contact angle values between left and right angles.

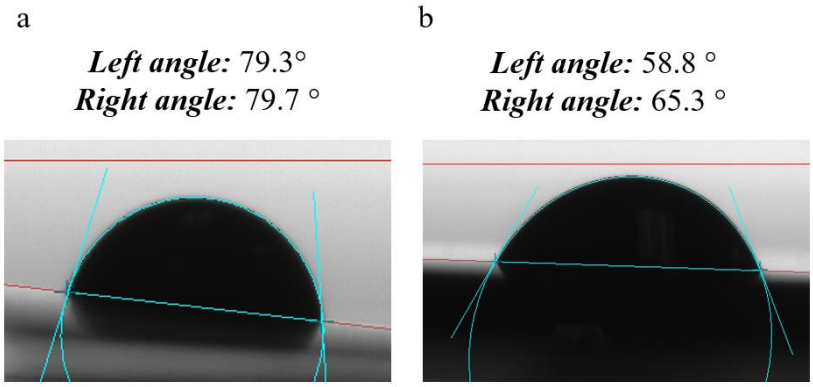

Figure 4.10 Contact angle captures of commercial Sepia melanin ink on paper substrate (a) and SiO_2 substrate (b).

4.4.3 Film characterization: SEM and profilometry

Images of films obtained from commercial Sepia melanin ink spin coated on gold-electrode-patterned SiO_2 substrates were taken by SEM (Figure 4.12). Images (a), (b), (d) and (e) highlight the presence of agglomerated Sepia granules forming blocks, as on picture (d). Importantly, the blocks are large enough to cover the channel (interelectrode space) (a). The size of Sepia melanin granules is about 100 - 260 nm for (c) and 230 nm for (f).

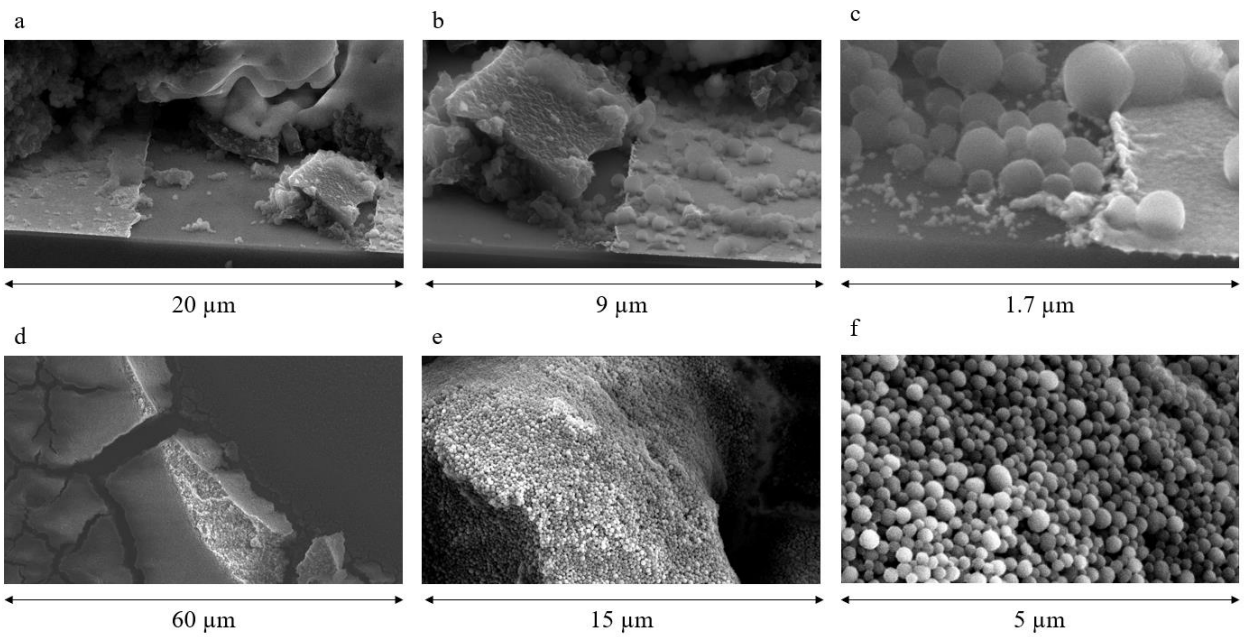

Figure 4.11 Spin coated commercial Sepia melanin ink film on Si/SiO_2 pictures by SEM with a length of (a) 20µm, (b) 9 µm, (c) 1.7 µm, (d) 60 µm, (e) 15 µm, (f) 5 µm.

Profilometry reveals that the average thickness for the five spin-coated films of commercial Sepia melanin is about 11 µm, with standard deviations between 4 and 9 µm depending on the samples (S1 to S5 are commercial ink spin coated samples, SN is natural ink with deionized water spin coated sample) (Figure 4.13). These deviations for each sample show an important irregularity of the surface. The standard deviation is associated to the profilometry values obtained for each sample measured from pad to pad of the electrode. The values used to estimate the standard deviation are from the first to the final inflexion point of the profile obtained, characterizing the beginning and the end of the spin coated film width. It is important to note that the high standard deviation is not only due to the surface irregularity but also to edge effects. Indeed, before spin coating, the electrode pads are covered with a tape to protect them and ensure they remain clean to prevent contact issues with the electrical measurements' probes. In this sense, due to the tape thickness, the local thickness at the edge of it is higher than for the rest of the film, as the ink tripped over the tape.

For samples prepared with the natural Sepia melanin ink, the average thickness is 4 µm and the deviation is lower as the natural ink was mixed with deionized water and magnetically stirred before spin-coating.

Compared to Sepia-shellac ink printed on paper, the thickness is about the same order of magnitude for commercial and natural inks, but the thickness for commercial ink is around two times higher. Commercial ink, then, might require to be magnetically stirred for both printing and spin coating.

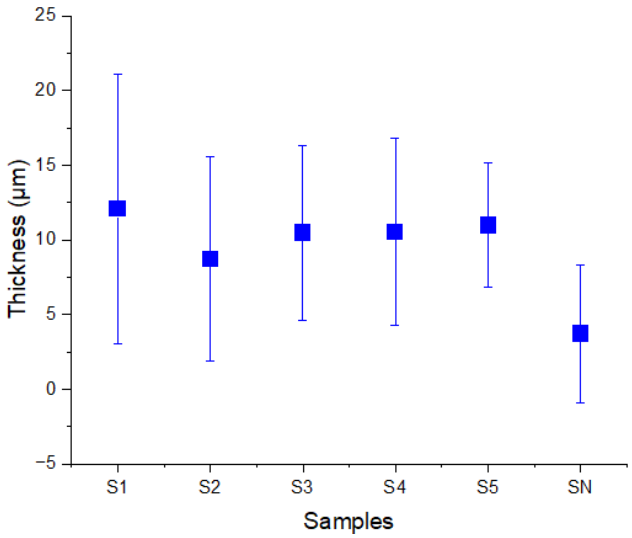

Figure 4.12 Thickness measured by profilometry of spin-coated commercial (S1 -S5) and natural (SN) Sepia melanin ink films on SiO_2 substrates.

4.4.4 Electrical response of natural and commercial in ambient conditions

Figure 4.14 shows the SiO_2 substrates photolithographically patterned with gold electrodes used in this work to carry out fundamental studies on the electrical properties of the films. Their fabrication and cleaning are well-established with respect to patterning and processing on paper substrates.

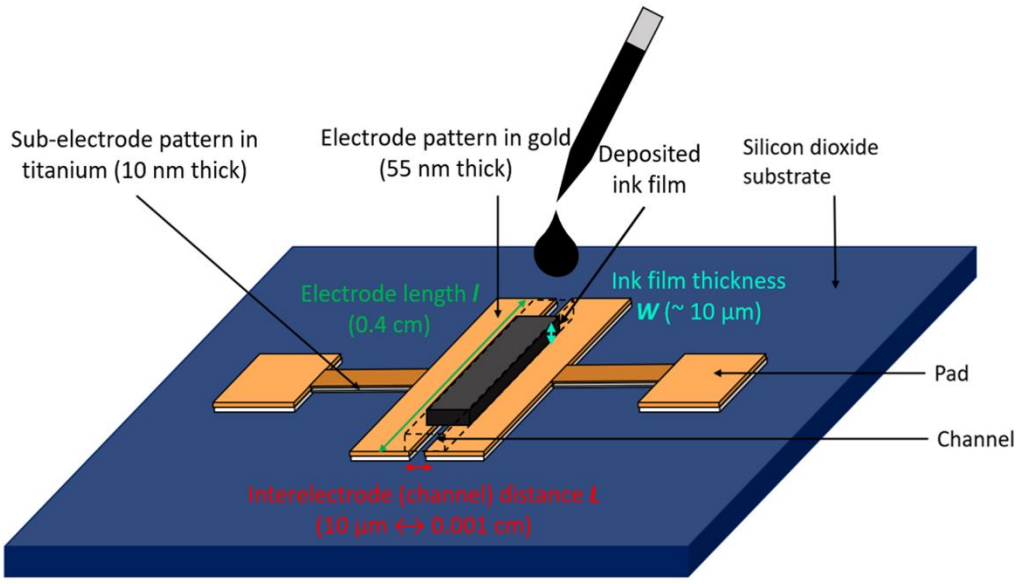

Figure 4.13 Scheme of the SiO_2 substrates patterned with gold electrodes used in this work for the measurements of the electrical reponse.

Concerning the electrical response of commercial and natural Sepia melanin inks, the first measurements were made through potentiostatic (I-t) and then current-potential (I-V) characteristics.

Figure 4.15 shows the potentiostatic measurements for commercial ink. Different shapes are observed for the curves. At low potential, for 0.1 V (Figure 4.14 (a)) and 0.5 V (Figure 4.14 (b)), a slight increase through time is observable. For higher potentials, 1 V (Figure 4.14 (c)) and 2 V (Figure 4.14 (d)), the current is stable or decreases. The time requested for the (ionic) electrical double layer to form could be key to understand the effect of the applied potential on the shapes of the curves.

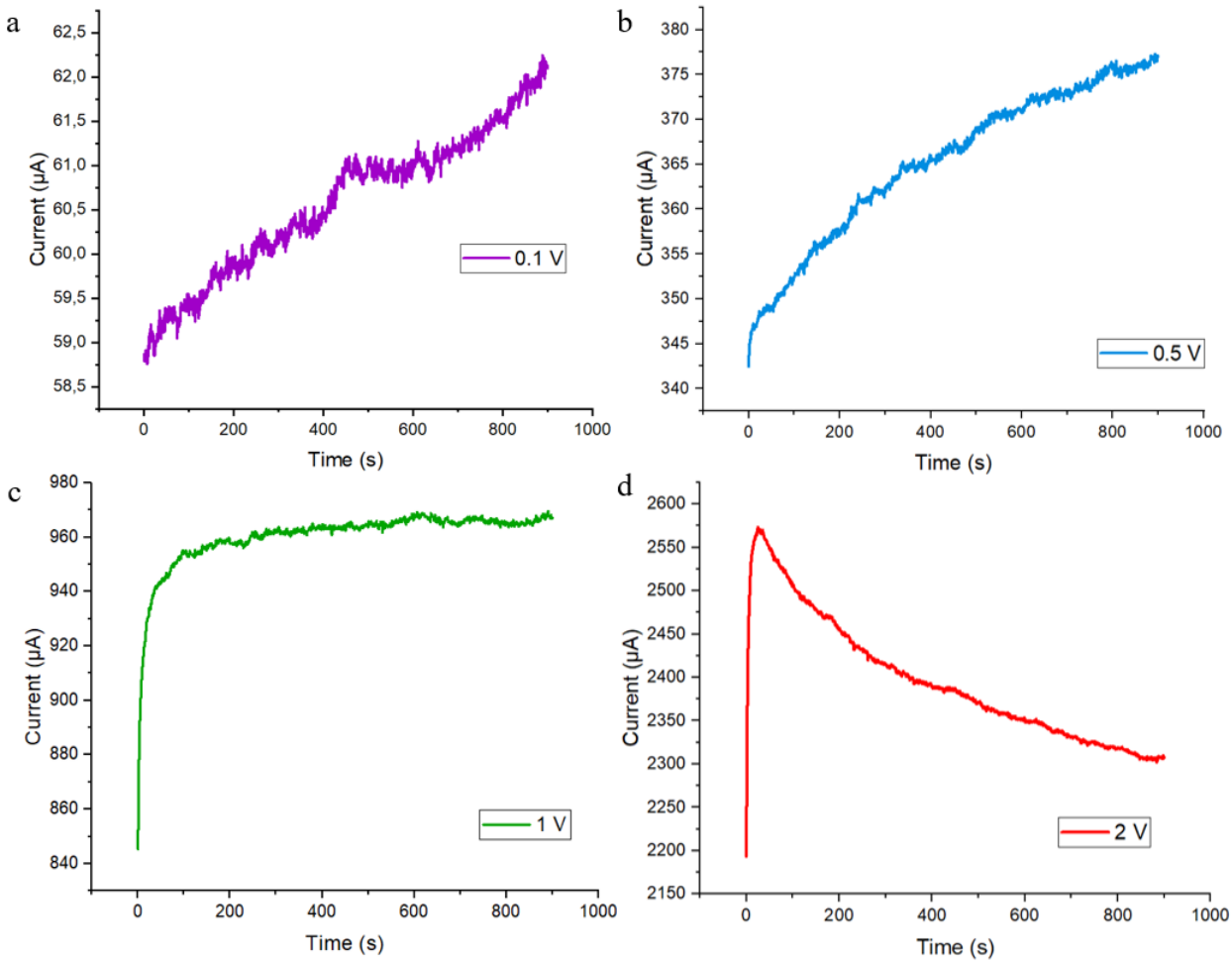

Figure 4.14 Potentiostatic measurements of spin-coated commercial Sepia melanin ink films on SiO_2 at 0.1 V, 0.5 V, 1 V and 2 V.

For the natural ink, the potentiostatic measurements give a different behavior from that observed with the commercial ink (Figure 4.15). Indeed, the current is maximum at the beginning of the scan and then it decreases. The higher ion concentration expected for the commercial ink with respect to the natural one can tentatively explain longer times to arrange the ions in the commercial ink case (or the higher applied potential needed to reach a constant, likely electronic, current).

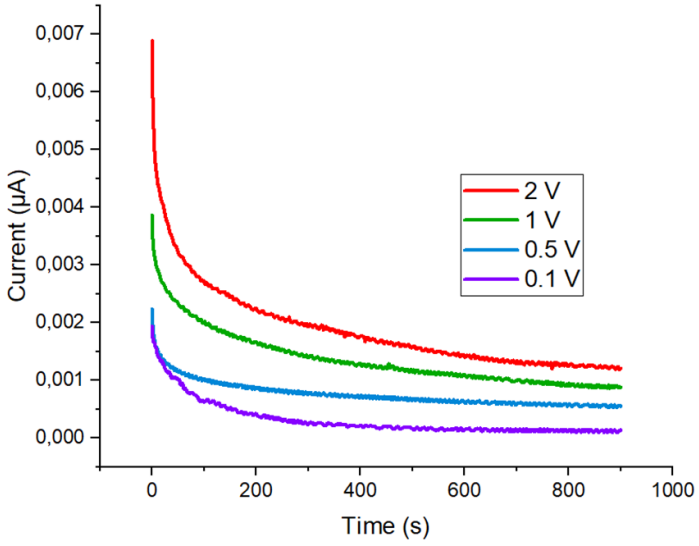

Figure 4.15 Potentiostatic measurements of spin coated natural Sepia melanin ink film on SiO_2 at 0.1 V, 0.5 V, 1 V and 2 V.

I-V measurements at different sweeping rates (1 mV/s, 10 mV/s and 100 mV/s, Figure 6.8) show a completely different behavior. The shape of the curves is ohmic for the commercial ink in the potential range investigated and for the sweeping rates considered. In agreement with [59] such behavior might be explained with a predominant electronic type of transport (instead of predominant ionic transport) for the commercial ink films. The very low currents recorder for the natural ink samples could be explained, tentatively, by the lack of water acting as glue between the Sepia melanin granules and between them and the SiO_2 surface in absence of the added, hygroscopic NaCl present in the commercial ink.

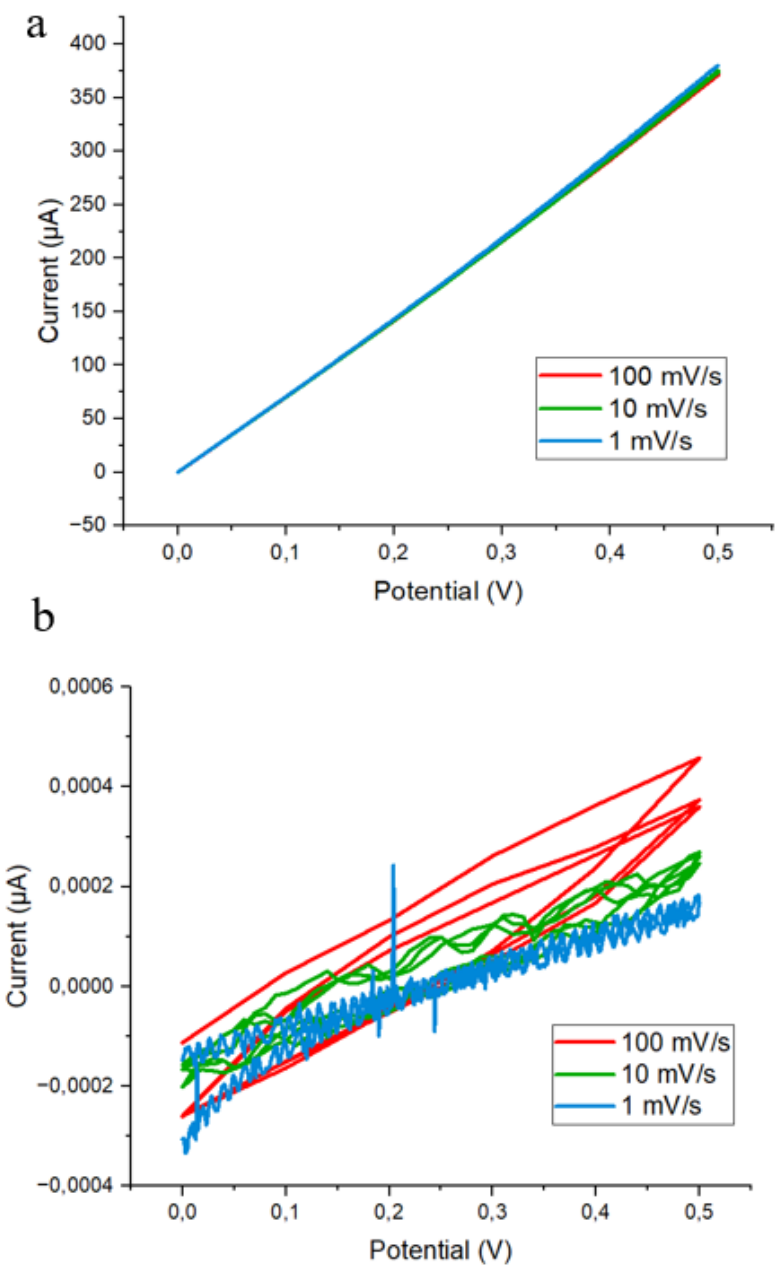

Figure 4.16 Current-potential characteristics of spin-coated commercial (a) and natural (b) Sepia melanin ink film on SiO_2.

The conductivity deduced at 0.5 V for commercial and natural ink respectively is about $2 \times 10^{-3}\, S.cm^{-1}$ and $10^{-9}\, S.cm^{-1}$ (Figure 4.17). The average thicknesses presented on Figure 4.13 and the electrode length (0.4 cm) on Figure 4.14 are used to calculate the cross-section area and then conductivity.

4.4.5 Influence of humidity on electrical response of commercial Sepia ink

Figure 4.17 shows the average current measured for five samples in different conditions and at different measurement rates.

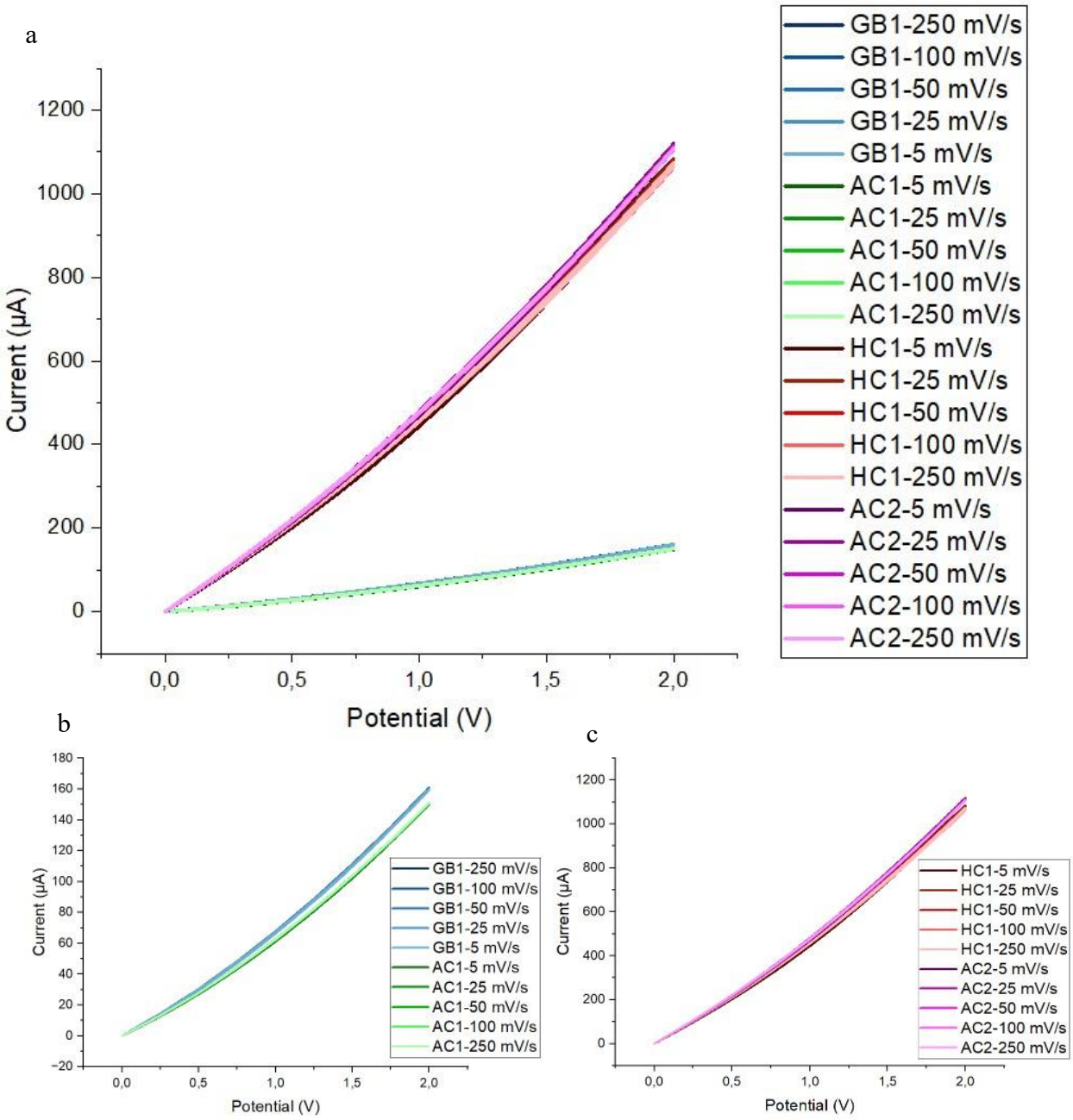

Figure 4.17 Current-potential (I-V) characteristics of spin-coated commercial Sepia melanin ink films on SiO_2 at 5, 25, 50, 100 and 250 mV/s in different conditions (a): first step in dry N_2 glove box (indicated as GB1) and second step in ambient conditions (indicated as AC1) (b), third step humidity chamber (indicated as HC1, 80 %RH) and fourth step ambient conditions, again (indicated as AC2) (c).

For commercial ink, measurements run in different conditions highlight current increase, after exposure in the humidity chamber at 80 % RH. Indeed, at 2 V, the current is about 150 µA both in dry (N_2 glove box) and ambient conditions, whereas in wet conditions the value is of about 1.1 mA, and it stays the same if the sample is taken back in ambient conditions.

The hygroscopicity of NaCl could explain why in ambient conditions after the wet conditions the current values do not change. Work is in progress to study the effect of the wet atmosphere on films made of natural ink. The conductivity for the initial step (GB1) and after the third step (HC1) is about $1.4 \times 10^{-4}\ S.cm^{-1}$ and $1.00 \times 10^{-3}\ S.cm^{-1}$. The increase due to the humidity is of one order of magnitude. In this sense, commercial Sepia ink, after further studies, could be an interesting bio-sourced material for moisture sensor organic electronic devices.

As for Sepia-shellac ink, commercial Sepia ink features a non-ohmic electrical response on a potential window between 0 and 2 V. Indeed, charge carrier trapping and potential electrode metal dissolution could be responsible for this behavior. The metal dissolution might be due to the presence of ions (e.g. sodium chloride) and water in the commercial Sepia ink.

CHAPTER 5 CONCLUSION AND PERSPECTIVES

Sepia melanin is a natural bio-pigment that develops functionalized indole-based building blocks, whose electronic conjugation confer to the pigment intriguing electrical properties of interest for sustainable, biodegradable organic electronics. The deposition of organic electronic materials by solution-based techniques, and notably, among them, printing, is interesting to limit, among others, the energy budget of manufactured devices since it can be carried out at room temperature, in ambient atmosphere conditions. Nevertheless, the limitation in terms of special resolution of printing techniques is way lower than that offered by more established patterning techniques used in microelectronics and nanoelectronics.

Sepia melanin-based ink rheology, wettability and printability on paper, investigated during this research project, indicated promising fabrication technologies for electronic devices. Similar preliminary results were observed for commercial Sepia melanin ink (not part of a printing formulation, without any chemicals added). These inks showed values of the electrical conductivity in the range of those typical of semiconductors, between $10^{-6}\ S.cm^{-1}$ and $10^{-3}\ S.cm^{-1}$. The findings, clearly still preliminary and at an exploration stage, open the path to bio-sourced organic electronic materials with, at least in principle, enhanced sustainability with respect to organic electronic materials synthesized in chemical laboratories and inorganic electronic materials including critical chemical elements.

The study of the electrical response of the films in different experimental conditions brought forth the effect of moisture in the atmosphere on the electrical conductivity. Moisture and thermal post-printing treatments led to enhanced conductivity for commercial Sepia melanin and Sepia-shellac ink. In this way, such inks represent an opportunity for biocompatible, flexible thermal or humidity sensing.

An important contribution this research project has made has been the acknowledgment of the important role that metal chemical elements, present during the biosynthesis of the natural materials, could have on the electrical response of the Sepia melanin-based films. The chemical composition has been studied through Neutron Activation Analysis.

The next step lies in pursuing electrical response studies with commercial and natural ink printed on paper. Mechanical, physicochemical tests (mechanochemistry) and the influence of humidity on the electrical response can help to optimize the biodegradation process. A crucial aspect to study is also the exact composition of the paper coating suspension used as it may contain potential non biodegradable or toxic compounds.

REFERENCES

[1] P. D. Department of Economic and Social Affairs, *World Population Prospects 2022*, no. 9. 2022. [Online]. Available: https://reliefweb.int/report/world/world-population-prospects-2022-summary-results?gclid=Cj0KCQjw3a2iBhCFARIsAD4jQB0ng8Sq2eudGc0yBXvWd6XsBPvncC7YrR1NkBv2zuSPvSs-Of1inX0aAhfLEALw_wcB

[2] A. Robert, "'Why Was the Industrial Revolution British?,'" *CEPR*, 2009. cepr.org/voxeu/columns/why-was-industrial-revolution-british

[3] U. S. F. & W. Service, "Rachel Carson (1907-1964) Author of the Modern Environmental Movement," *FWS.gov*. https://www.fws.gov/staff-profile/rachel-carson-1907-1964-author-modern-environmental-movement

[4] B. R. Keeble, "The Brundtland Report: 'Our Common Future,'" *Medicine and War*, vol. 4, no. 1. pp. 17–25, 1988. doi: 10.1080/07488008808408783.

[5] J. Pelenc, "Weak Sustainability versus Strong Sustainability."

[6] HLPF, "Global Sustainable Development Report Advance unedited version," *United Nations*, no. June, pp. 1–24, 2011, [Online]. Available: https://sustainabledevelopment.un.org/content/documents/1758GSDR 2015 Advance Unedited Version.pdf

[7] V. Forti, C. P. Balde, R. Kuehr, and G. Bel, "The Global E-waste Monitor 2020: Quantities, flows and the circular economy potential," *Quant. flows, Circ. Econ. potential*, pp. 1–119, 2020, [Online]. Available: http://ewastemonitor.info/

[8] X. Yan, "2018_Pnas_Si_Spe," *Proc. Natl. Acad. Sci.*, vol. 120, p. 2017, 2017, doi: 10.1073/pnas.

[9] C. Santato and P. J. Alarco, "The Global Challenge of Electronics: Managing the Present and Preparing the Future," *Adv. Mater. Technol.*, vol. 7, no. 2, Feb. 2022, doi: 10.1002/admt.202101265.

[10] R. McNeill, R. Siudak, J. Wardlaw, and D. Weiss, "Electronic Conduction in Polymers. I. The Chemical Structure of Polypyrrole," *Aust. J. Chem.*, vol. 16, no. 6, p. 1056, 1963, doi:

10.1071/CH9631056.

[11] H. Heeger, Alan J. ; MacDiarmid, Alan G. ; Shirakawa, “Advanced Information - The Nobel Prize in Chemistry 2000,” *Nobel Media AB 2019*, pp. 1–16, 1974, doi: 10.1007/978-1-84996-290-2.

[12] “Alan J. Heeger, Alan G. MacDiarmid, and Hideki Shirakawa,” *Macromolecules*, vol. 35, no. 4, pp. 1137–1139, Feb. 2002, doi: 10.1021/ma0118973.

[13] H. Hoppe and N. S. Sariciftci, “Nanostructure and Nanomorphology Engineering in Polymer Solar Cells,” in *Nanostructured Materials for Solar Energy Conversion*, Elsevier, 2006, pp. 277–318. doi: 10.1016/B978-044452844-5/50011-1.

[14] L. Deng, Z. Liu, and L. Li, “Hybrid nanocomposites for imaging-guided synergistic theranostics,” in *Nanomaterials for Drug Delivery and Therapy*, Elsevier, 2019, pp. 117–147. doi: 10.1016/B978-0-12-816505-8.00017-5.

[15] A. Sudheshwar, N. Malinverno, R. Hischier, B. Nowack, and C. Som, “The need for design-for-recycling of paper-based printed electronics – a prospective comparison with printed circuit boards,” *Resour. Conserv. Recycl.*, vol. 189, no. October 2022, p. 106757, Feb. 2023, doi: 10.1016/j.resconrec.2022.106757.

[16] A. Camus, M. Reali, and C. Santato, “Advances in high-resolution printed transistors: The case of bio-sourced organic materials,” *Current Opinion in Green and Sustainable Chemistry*, vol. 34. Elsevier B.V., Apr. 01, 2022. doi: 10.1016/j.cogsc.2022.100594.

[17] B. Lüssem, C. M. Keum, D. Kasemann, B. Naab, Z. Bao, and K. Leo, “Doped Organic Transistors,” *Chemical Reviews*, vol. 116, no. 22. American Chemical Society, pp. 13714–13751, Nov. 23, 2016. doi: 10.1021/acs.chemrev.6b00329.

[18] F. Torricelli, I. Alessandri, E. Macchia, I. Vassalini, M. Maddaloni, and L. Torsi, “Green Materials and Technologies for Sustainable Organic Transistors,” *Advanced Materials Technologies*, vol. 7, no. 2. John Wiley and Sons Inc, Feb. 01, 2022. doi: 10.1002/admt.202100445.

[19] W. D. Callister and D. G. Rethwisch, “Materials Science and Engineering, An Introduction,” 2018. [Online]. Available: www.wiley.com/go/permissions.

[20] C. Kittel, *Introduction to Solid State Physics Charles Kittel*, vol. 8. 2005.

[21] H. Kleemann, K. Krechan, A. Fischer, and K. Leo, "A Review of Vertical Organic Transistors," *Advanced Functional Materials*, vol. 30, no. 20. Wiley-VCH Verlag, May 01, 2020. doi: 10.1002/adfm.201907113.

[22] T. Schuman, A. Karlsson, J. Larsson, M. Wikström, and M. Rigdahl, "Characteristics of pigment-filled polymer coatings on paperboard," *Prog. Org. Coatings*, vol. 54, no. 4, pp. 360–371, Dec. 2005, doi: 10.1016/j.porgcoat.2005.06.017.

[23] A. Blayo and B. Pineaux, "Printing processes and their potential for RFID printing," *ACM Int. Conf. Proceeding Ser.*, vol. 121, pp. 27–30, 2005, doi: 10.1145/1107548.1107559.

[24] Y. Yuan *et al.*, "Shellac: A promising natural polymer in the food industry," *Trends in Food Science and Technology*, vol. 109. Elsevier Ltd, pp. 139–153, Mar. 01, 2021. doi: 10.1016/j.tifs.2021.01.031.

[25] M. Irimia-Vladu, "'Green' electronics: Biodegradable and biocompatible materials and devices for sustainable future," *Chemical Society Reviews*, vol. 43, no. 2. Royal Society of Chemistry, pp. 588–610, Jan. 21, 2014. doi: 10.1039/c3cs60235d.

[26] W. Cao *et al.*, "Unraveling the structure and function of melanin through synthesis," *J. Am. Chem. Soc.*, vol. 143, no. 7, pp. 2622–2637, Feb. 2021, doi: 10.1021/jacs.0c12322.

[27] P. Meredith and T. Sarna, "The physical and chemical properties of eumelanin," *Pigment Cell Research*, vol. 19, no. 6. pp. 572–594, Dec. 2006. doi: 10.1111/j.1600-0749.2006.00345.x.

[28] M. Reali, C. Santato, and F. Cicoira, "Title: Eumelanin for Organic Electronics : Film Formation and Transport Physics Génie physique," Polytechnique, 2021.

[29] *Melanins: Functions, Biotechnological Production, and Applications*. Springer International Publishing, 2023. doi: 10.1007/978-3-031-27799-3.

[30] A. Büngeler, B. Hämisch, K. Huber, W. Bremser, and O. I. Strube, "Insight into the Final Step of the Supramolecular Buildup of Eumelanin," *Langmuir*, vol. 33, no. 27, pp. 6895–6901, Jul. 2017, doi: 10.1021/acs.langmuir.7b01634.

[31] C. M. R. Clancy and J. D. Simon, "Ultrastructural organization of eumelanin from Sepia

officinalis measured by atomic force microscopy," *Biochemistry*, vol. 40, no. 44, pp. 13353–13360, Nov. 2001, doi: 10.1021/bi010786t.

[32] A. Mbonyiryivuze *et al.*, "Morphological and Chemical Composition Characterization of Commercial Sepia Melanin," *Am. J. Nanomater.*, vol. 3, no. 1, pp. 22–27, Jun. 2015, doi: 10.12691/ajn-3-1-3.

[33] E. Di Mauro, D. Rho, and C. Santato, "Biodegradation of bio-sourced and synthetic organic electronic materials towards green organic electronics," *Nat. Commun.*, vol. 12, no. 1, Dec. 2021, doi: 10.1038/s41467-021-23227-4.

[34] R. Argenziano, M. L. Alfieri, N. Gallucci, G. D'Errico, L. Panzella, and A. Napolitano, "A Model Eumelanin from 5,6-Dihydroxyindole-2-Carboxybutanamide Combining Remarkable Antioxidant and Photoprotective Properties with a Favourable Solubility Profile for Dermo-Cosmetic Applications," *Int. J. Mol. Sci.*, vol. 24, no. 4, p. 4241, Feb. 2023, doi: 10.3390/ijms24044241.

[35] J. Mcginness, P. Corry, and P. Proctor, "Amorphous semiconductor switching in melanins," *Science (80-.).*, vol. 183, no. 4127, pp. 853–855, 1974, doi: 10.1126/science.183.4127.853.

[36] A. B. Mostert, "The importance of water content on the conductivity of biomaterials and bioelectronic devices," *Journal of Materials Chemistry B*, vol. 10, no. 37. pp. 7108–7121, 2022. doi: 10.1039/d2tb00593j.

[37] M. Reali, P. Saini, and C. Santato, "Electronic and protonic transport in bio-sourced materials: A new perspective on semiconductivity," *Materials Advances*, vol. 2, no. 1. pp. 15–31, 2021. doi: 10.1039/d0ma00579g.

[38] cPhD; P. P. Mario Magarelli*, Químico, Q. C. Renieri, and Biólogo, "Purification , characterization and analysis of sepia melanin from commercial sepia ink (Sepia Officinalis) Purificación , caracterización y análisis de la melanina de sepia a partir de la tinta de sepia (Sepia Officinalis)," *Rev. CES Med. Vet. y Zootec.*, vol. 5(2), pp. 18–28, 2010.

[39] M. Abdollahi Neisiani, M. Latifi, J. Chaouki, and C. Chilian, "Novel approach in k0-NAA for highly concentrated REE Samples," *Talanta*, vol. 180, pp. 403–409, Apr. 2018, doi: 10.1016/j.talanta.2017.11.026.

[40] J. Ene-Parent, "Titre: Title: Analyse par activation neutronique de la charpie de sécheuses,"

2000. [Online]. Available: https://publications.polymtl.ca

[41] S. Zahoor, W. Abdul-Kader, H. Ijaz, A. Khan, Z. Saeed, and S. Muzaffar, “A Combined VSM and Kaizen Approach for Sustainable Continuous Process Improvement,” *Int. J. Ind. Eng. Oper. Manag.*, vol. 01, no. 02, Dec. 2019, doi: 10.46254/j.ieom.20190203.

[42] W. W. Sampson, “Grammage dependence of paper thickness | Request PDF,” *Appita J.*, vol. 72, no. 1, pp. 29–39, 2019, Accessed: Jul. 29, 2023. [Online]. Available: https://research.manchester.ac.uk/en/publications/grammage-dependence-of-paper-thickness

[43] ISO, “ISO 536:1995 Paper and board — Determination of grammage,” *ISO_536_2012.pdf*, no. 121562, 1997, Accessed: Jul. 29, 2023. [Online]. Available: https://www.iso.org/standard/60352.html

[44] “Thickness (caliper of paper, paperboard, and combined board, Test Method TAPPI/ANSI T 411 om-21.” Accessed: Jul. 29, 2023. [Online]. Available: https://imisrise.tappi.org/TAPPI/Products/01/T/0104T411.aspx

[45] “International Standard ISO 535 – Paper and Board Determination of Water Absorptiveness-Cobb method.” Accessed: Jul. 29, 2023. [Online]. Available: https://www.iso.org/standard/80320.html

[46] R. Tadmor, “Line energy and the relation between advancing, receding, and Young contact angles,” *Langmuir*, vol. 20, no. 18, pp. 7659–7664, 2004, doi: 10.1021/la049410h.

[47] J. Zhao and X. Liu, “Electron microscopic methods (TEM, SEM and energy dispersal spectroscopy),” in *Reference Module in Earth Systems and Environmental Sciences*, Elsevier, 2022. doi: 10.1016/b978-0-12-822974-3.00013-6.

[48] A. M. Donald, “The use of environmental scanning electron microscopy for imaging wet and insulating materials,” *Nat. Mater.*, vol. 2, no. 8, pp. 511–516, 2003, doi: 10.1038/nmat898.

[49] D. C. J. Savile Bradbury, “Scanning electron microscope (SEM) | Definition, Images, Uses, Advantages, & Facts | Britannica,” *The Editors of Encyclopaedia Britannica*, 2023. https://www.britannica.com/technology/scanning-electron-microscope (accessed Aug. 03, 2023).

[50] K. Wasmund, M. Mußmann, and A. Loy, “The life sulfuric: microbial ecology of sulfur cycling in marine sediments,” *Environmental Microbiology Reports*, vol. 9, no. 4. pp. 323–344, Aug. 2017. doi: 10.1111/1758-2229.12538.

[51] C. D. Derby, “Cephalopod ink: Production, chemistry, functions and applications,” *Marine Drugs*, vol. 12, no. 5. pp. 2700–2730, May 12, 2014. doi: 10.3390/md12052700.

[52] S. J. Parry, “Activation Analysis - Neutron Activation,” in *Encyclopedia of Analytical Science: Second Edition*, Elsevier, 2004, pp. 1–10. doi: 10.1016/B0-12-369397-7/00002-9.

[53] T. Shende, V. J. Niasar, and M. Babaei, “An empirical equation for shear viscosity of shear thickening fluids,” *J. Mol. Liq.*, vol. 325, p. 115220, Mar. 2021, doi: 10.1016/j.molliq.2020.115220.

[54] A. Yahia, S. Mantellato, and R. J. Flatt, “Concrete rheology: A basis for understanding chemical admixtures,” *Sci. Technol. Concr. Admixtures*, pp. 97–127, Jan. 2016, doi: 10.1016/B978-0-08-100693-1.00007-2.

[55] W. K. Wilsoin and E. J. Parks, “An Analysis of the Aging of Paper: Possible Reactions and their Effects on Measurable Properties,” *Restaurator*, vol. 3, no. 1–2, pp. 37–62, 1979, doi: 10.1515/rest.1979.3.1-2.37.

[56] H. Wang, B. Yu, S. Jiang, L. Jiang, and L. Qian, “UV/ozone-assisted tribochemistry-induced nanofabrication on Si(100) surfaces,” *RSC Adv.*, vol. 7, no. 63, pp. 39651–39656, 2017, doi: 10.1039/c7ra07198a.

[57] J. Gärd and C. Kemiteknik, “The Influence of Fibre Curl on the Shrinkage and Strength Properties of Paper MASTER’S THESIS 257, Luleå University of Technology, Luleå , Sweden,” 2002.

[58] O. D. Jurchescu and T. T. M. Palstra, “Crossover from one- to two-dimensional space-charge-limited conduction in pentacene single crystals,” *Appl. Phys. Lett.*, vol. 88, no. 12, 2006, doi: 10.1063/1.2187442.

[59] M. Reali *et al.*, “Eumelanin: From molecular state to film,” *J. Phys. Chem. C*, vol. 125, no. 6, pp. 3567–3576, Feb. 2021, doi: 10.1021/acs.jpcc.0c10063.

APPENDIX A NEUTRON ACTIVATION ANALYSIS AND SEPIA MELANIN EXTRACTION PROTOCOLS

SLOWPOKE NAA LABORATORY

1. Procedure for the Determination of Elemental Concentration by Neutron Activation Analysis

General description:

To determine the elemental concentration in organic and inorganic samples, around 0.1 to 5.0 grams are usually sampled from the bulk sample. The sample is weighed into a 1.4 mL or 7 mL polyethylene vial, and inserted in a polyethylene irradiation vial. The entire sample is bombarded with neutrons from a nuclear reactor and a fraction of the element atoms are converted to radioactive isotopes. These radioactive atoms subsequently emit their surplus energy in the form of gamma rays, which are then detected. The number of gamma rays detected is proportional to the amount of the element in the sample. The exact amount of the element is calculated by comparing with a standard prepared from an element solution of known concentration.

Equipment used:

SLOWPOKE nuclear reactor, Atomic Energy of Canada Limited

Pneumatic transfer system

Germanium semiconductor gamma-ray detector, Ortec model GEM55185

Multichannel analyzer, Ortec model DSPEC Pro

Balance, Sartorious model MSU 124-S, precision 0.0001g

Procedure:

- Record the external sample ID in the logbook and assign the internal sample ID in the logbook and on the sample package.
- Write the internal sample ID on the irradiation vials containing the sample.
- Weigh the sample; the result will be expressed in ppm (μg/g).
- Place the sample in a 7 mL irradiation polyethylene vial (rabbit).
- Using the reactor's pneumatic transfer system, irradiate the sample for 30 to 600 sec for short half-life (or for 3 to 5h for average and long half-life elements) in one of the inner irradiation site (#1 to #5) at an average thermal neutron flux of 5 x 10^{11}/cm^2/s (which varies between 4.43 and 5.58 x 10^{11}/cm^2/s as a function of the position of the sample in the irradiation site).
- Allow the radioactivity to decay for 300 sec (or for several days for average and long half-life elements).
- Count the sample for 10-20 min (or for 5-10 hours for average and long half-life elements) at a distance of 0.16 cm, 3 cm or 10 cm from the detector (position 1, 2 or 3).
- Record the gamma-ray spectrum with a file name containing the sample ID.
- Calculate the amount of the elements, in ppm, using the EPAA software to read the gamma-ray spectrum and perform the calculation. The calculation involves determining the photo peak area, correcting for analyzer dead time and dividing by the element sensitivity previously measured with a standard.
- Short half-life elements: F, Al, Cl, Mg, Ti, Mn, Si, S, Ca, V, Se, Br, I, Ba, Cu, In, Sn, U;
- Medium half-life elements: Na, K, Zn, As, Sb, Br, Mo, La, Au, W;
- Long half-life elements: Fe, Ni, Co, Cs, Cr, Sc, Zn, Se, Rb, Zr, Ag, Cd, Hf, Th, U.

Accuracy:

5% of the measured value or better.

Range of applicability:

0.02 ppm to 100%.

Calibration standards:

The system was calibrated with standard Specpure solutions of 1000 ppm element concentration, which was specified by the manufacturer as being more than 99% pure. 1 mL solutions were pipetted onto 15 mm x 800 mm rectangular paper filter, previously determined to be free from gold, and air dried. These were enclosed in 1.4 mL

polyethylene irradiation vials. These standards were used to determine the sensitivity of the procedure (in counts/μg).

Quality assurance:

Measurements carried out over several years have shown the reactor neutron flux and the detector efficiency to be reproducible to 1%. Thus, analyses carried out with the measured sensitivity constant will not suffer from loss of accuracy greater than 1% due to variations of these parameters. This is verified routinely by the analysis of a quality control standard containing 30 μg of the element to be analysed. The measured value must be within 2 SD of the expected value.

2. Sepia melanin extraction refined version, Spring 2021

Laboratory: J-3312

1. Take the cuttlefish ink from the freezer, let it defreeze for 30 minutes, then shake it vigorously
2. Take a big baker and place in it 300 g of raw cuttlefish ink.
3. Preparing HCl 2M: pour 100 mL of HCl (37%) into 500 mL of deionized water (DO NOT DO THE OPPOSITE!!! NEVER ADD WATER TO ACIDS!). Then, slowly pour the HCl 2M into the baker with the raw ink as in step 2 in order to prepare the ink for Centrifugation and Wash suspension; from now on, “ink+acid” will be called “slurry”.
4. Stir the slurry for 24hr with a magnet (decide the rpm such that the suspension is vigorously shaken but there is no vortex), ideally keeping the slurry at 10 °C.
5. STRONGLY SUGGESTED: Also prepare 600 mL of HCl 0.5 M for the next steps and keep it ready in closed, labelled glass containers. To prepare HCl 0.5 M: pour 25 mL of HCl 37% into 575 mL of deionized water (DO NOT DO THE OPPOSITE!!! NEVER ADD WATER TO ACIDS!)

6. STRONGLY SUGGESTED: Also prepare the buffer solution for the next steps and keep it in closed, labelled glass containers. To prepare the buffer solution: (i) pour 4 µL of Monobasic Sodium Phosphate in 38 mL of deionize water; (ii) pour 65 mL of Dibasic Sodium Phosphate in 97 mL of deionized water; (iii) mix (i) and (ii) in 200 mL of deionized water.
7. Once the 24 h stirring of the initial slurry are completed: Distribute the suspension ink + 2M HCl acid in the
    1. If the total volume ≤280ml, 8 small cylindrical containers (280ml/8=35ml) for the small centrifuge
    2. If the total volume >280ml, 6 cylindrical containers for the big centrifuge (370 ml maximum each).

ATTENTION: Do not fill the bottles one by one, but fill the 6 bottles gradually (first 30 ml in each bottle, then other 30 ml in each bottle and so on).

8. The steps of the centrifugation (10000 rpm at 5 °C, the duration can be 15 min or 25 min or 30 min) are the following:
    1. Step with 2 M HCl

i. Shake vigorously the containers
ii. Measure the pH
iii. Equalize the weights
iv. Wash suspension
v. Weigh the buckets
vi. Centrifuge 15 min

2. wash-suspension with 0.5 M HCl solution, 1

i. Take a picture
ii. Remove the liquid
iii. Add the new solvent (0.5 M Cl)
iv. Scratch the solid sticking to the walls
v. Equalize the weights

v. Wash suspension

v. Weigh the buckets

v. Centrifuge 15 min

3. wash-suspension with 0.5 M HCl solution, 2

1. Take a picture
2. Measure the pH
3. Remove the liquid
4. Add the new solvent (0.5 M Cl)
5. Scratch the solid sticking to the walls
6. Equalize the weights
7. Wash suspension
8. Weigh the buckets
9. Centrifuge 15 min

4. wash-suspension with 0.5 M HCl solution, 3

1. Take a picture
2. Measure the pH
3. Remove the liquid
4. Add the new solvent (0.5 M Cl)
5. Scratch the solid sticking to the walls
6. Equalizing the weights
7. Wash suspension
8. Weigh the buckets
9. Centrifuge 15 min

5. wash-suspension with water, 1

1. Take a picture
2. Measure the pH
3. Remove the liquid
4. Add the new solvent (water)
5. Scratch the solid sticking to the walls
6. Equalize the weights
7. Wash suspension

8. Weigh the buckets (only for the small centrifuge)
9. Centrifuge 15 min

ATTENTION: If some DI water is left, cover it with cellophane film/parafilm, it may be contaminated by the following steps

6. Wash-suspension with the Buffer (in 500 mL, 4 μL of Monobasic Sodium Phosphate in 38 mL of deionized water, 65 mL of Dibasic Sodium Phosphate in 97 mL of deionized water, then mix all in 200ml deionized water)

1. Take a picture
2. Measure the pH
3. Remove the liquid
4. Add the new solvent (buffer)
5. Scratch the solid sticking to the walls
6. Equalize the weights
7. Wash suspension
8. Weigh the buckets
9. Centrifuge 25 min

7. wash-suspension with water, 2

1. Take a picture
2. Measure the pH
3. Remove the liquid
4. Add the new solvent (water)
5. Scratch the solid sticking to the walls
6. Equalize the weights
7. Wash suspension
8. Weigh the buckets
9. Centrifuge 25 min

8. wash-suspension with water, 3

1. Take a picture
2. Measure the pH
3. Remove the liquid

4. Add the new solvent (water)
5. Scratch the solid sticking to the walls
6. Equalize the weights
7. Wash suspension
8. Weigh the buckets
9. Centrifuge 25 min

9. wash-suspension with ethanol

1. Take a picture
2. Measure the pH
3. Remove the liquid
4. Add the new solvent (ethanol)
5. Scratch the solid sticking to the walls
6. Equalize the weights
7. Wash suspension
8. Weigh the buckets
9. Centrifuge 15 min

10. wash-suspension with ethyl acetate

1. Take a picture
2. Remove the liquid
3. Add the new solvent (ethyl acetate)
4. Equalize the weights
5. Wash suspension
6. Weigh the buckets (only for the small centrifuge)
7. Centrifuge 15 min

11. wash-suspension with water, 4

1. Take a picture
2. Remove the liquid
3. Add the new solvent (water)
4. Scratch the solid sticking to the walls
5. Equalize the weights
6. Wash suspension

7. Weigh the buckets (only for the small centrifuge)
8. Centrifuge 30 min

12. wash-suspension with water, 5

1. Take a picture
2. Remove the liquid
3. Add the new solvent (water)
4. Scratch the solid sticking to the walls
5. Equalize the weights
6. Wash suspension
7. Weigh the buckets (only for the small centrifuge)
8. Centrifuge 30 min

13. wash-suspension with water, 6

1. Take a picture
2. Remove the liquid
    3. Add the new solvent (water)
4. Scratch the solid sticking to the walls
5. Equalize the weights
6. Wash suspension
7. Weigh the buckets (only for the small centrifuge)
8. Centrifuge 30 min

14. wash-suspension with water, 7

1. Take a picture
2. Remove the liquid
    3. Add the new solvent (water)
    4. Scratch the solid sticking to the walls
    5. Equalize the weights
6. Wash suspension
7. Weigh the buckets (only for the small centrifuge)
8. Centrifuge 30 min

9. 24 hr lyophilization to remove all solvent (contact Benoit Liberelle, benoit.liberelle@polymtl.ca)

A very thin black product was obtained at the end of the procedure.

“EQUILIZING THE WEIGHTS” STEP (20 minutes)

The 8(6) containers will be put in 2 buckets in the centrifuge. It is absolutely crucial that the 2 buckets have the same weight, so 4 samples have to be named “A” and 4 others “B” (for the sake of clarity, we’ll say A 1,2,3,4 and B 1,2,3,4). So:

- For samples 1, 2, 3 of A and B: Tare the scale to the sample A1, and be sure that all the other samples do not differ by more than 100mg from it. If so, remove some liquid adding it to the samples A4 or B4 or add some liquid from the samples A4 or B4.
- For the samples 4 of A and B: make their weight equal, mark them with an “X” (as their weight may differ from the other 3 of their group).

“REMOVE LIQUID” STEP (20 minutes)

After the centrifugation:

- Remove the supernatant, until you leave only the solid, for each sample. If the solid accumulated on the bottom and on one side, you can tilt the sample and take the liquid from the empty side.

“ADD LIQUID” STEP (20 minutes)

- Add the necessary amount of the solvent to each sample to reach the initial volume (only for HCl 0.5 M the first time do 3 up and downs with the pipette to be sure that after the dilution the solution is well mixed)

“WASH SUSPENSION” STEP (30 minutes for the first centrifugation, 20 minutes for the following centrifugations until the one with the buffer included, then for the following centrifugations 15 minutes)

- Shake the samples
- Put the samples one by one on the vortex (hold it with 1-2 fingers from the top, never from the sides otherwise you’ll break the machine).

- Put the samples in the ultrasonic bath for 25 minutes for the first centrifugation, 15 minutes for the following centrifugations until the one with the buffer included, then for the following centrifugations 10 minutes. Add ice to the ultrasonic bath before putting the sample holders. Shake them every 5 minutes.
- Remove the samples from the ultrasonic bath and dry the samples externally

"WEIGH THE BUCKETS" STEP (5 minutes, only for the small centrifuge)

- For the small centrifuge: weight the 2 buckets: the difference should be < 350 mg.

CENTRIFUGE STEP (15 minutes)

For the small centrifuge

- Turn on the centrifuge on its back
- Choose program 6 (it has 4696g=5000 rpm speed, it is the maximum)
- Set "Time" (15 minutes)
- Set Temperature (5°C)
- Leave "Acc" and "Dec" to 9
- Open it and check that the 2 green containers are ok.
- Put the buckets in being sure that the two samples marked with an "X" are the closet the centrifuge center.
- Click on "Start": with one hand, be ready on the button "Stop", with the other check the vibrations from the top of the centrifuge.

For the big centrifuge

- Turn it on on the right
- Register on the paper on its top
- Put your rotor
- Put your samples
- Check that there is the seal on the rotor cap, close turning clockwise
- Enter the
    - Rotor
    - Rpm

    - Time
    - Temperature
- Click on “Enter”
- Click on “Start”
- Stay there until it reaches 10000 rpm
- At the end of the day, clean and leave the door open.

LYOPHILIZATION

Freeze your samples at -80°C.

Never leave the samples horizontal, always place them slightly tilted upwards.

1. Turn on the fan
2. Turn on the lyophilisation machine on its back. If there is an alarm call Benoit.
3. Go on “Automatic Mode”->Maintenance->1
4. Manual mode:
    1. Manual Freeze Setpoint: -40°C
    2. Manual Heating Setpoint: -20°C
    3. Vacuum: 100mTorr
    4. Defrost: 50°C
    5. Defrost time: 60 min
    6. Vacuum Release Time: 1 minute
5. Synoptic
6. Check that everything inside is dry and clean (no dust)
7. Click on “Freeze” 3 seconds to start cooling the metal shelves. If after clicking on « freeze » you have the message " Automatic Mode unavailable" then click again on « Shelf CTR", and then click again on “Freeze" (sometimes "Shelf CTR" seems to be off when it is actually on).
8. Leave it on for 1 hour (to let the shelves get to -30°C)
9. Click on “Condenser” for 3 seconds
10. Click on “Vacuum” for 3 seconds
11. Push the door to “help” to make the vacuum

12. Check that the pressure is decreasing
13. Click for 3 seconds on “Shelf CTRL”
14. Check that there is the message “Manual Mode + Heat -> -20°C”
15. Click for 3 seconds on “Vac CTRL”. It has to get to P+100mTorr
16. To stop:
    1. Click on “Vacuum CTRL” for 3 seconds
    2. Click on “Shelf CTR” for 3 seconds
    3. Click on “Vacuum for” for 3 seconds
    4. Click on “Condenser” for 3 seconds
    5. Vacuum Release
17. Wait 2 minutes, then open the door
18. Click for 3 seconds on “Defrost” and unplug the fan
19. When the “Defrost” light is off, dry the water on the bottom with a brown paper
20. Leave the door almost open for 1 day so that all the humidity can leave
21. Turn off the machine on its back

References:

Magarelli, M.; Passamonti, P.; Renieri, C. Purification , Characterization and Analysis of Sepia Melanin from Commercial Sepia Ink (Sepia Officinalis) Purificación , Caracterización Y Análisis de La Melanina de Sepia a Partir de La Tinta de Sepia (Sepia Officinalis) Resumen. *Rev. CES Med. Vet. y Zootec.* **2010**, *5*, 18–28.

Fort the part with ethanol and ethyl acetate: M. Araujo, J.R. Xavier, C.D. Nunes, P.D. Vaz, M. Humanes, Marine sponge melanin: A new source of an old biopolymer, Struct. Chem. 23 (2012) 115–122. doi:10.1007/s11224-011-9843-7